SLAC-PUB-1643
August 1975
(T/E)

e^+e^- INTERACTIONS*

Harvey L. Lynch

Stanford Linear Accelerator Center
Stanford University, Stanford, California 94305

(Lectures delivered at Cargèse Summer School, Cargèse, France, July 1975.)

* Work supported by U. S. Energy Research and Development Administration.

INTRODUCTION

The field of e^+e^- interactions has provided a great deal of excitement in the past few years.[1-9] Primarily, interest has centered around the reaction $e^+e^- \rightarrow$ hadrons. This reaction is particularly attractive because we believe in electromagnetic perturbation theory, which implies that the cross section for hadron production is dominated by one photon annihilation of the electron and positron. As a consequence of the single photon intermediate state the quantum numbers of the hadronic system are well defined, a nearly unique situation in hadron physics. The hadronic state must share the spin, parity, and charge conjugation assignment of the photon, $J^{PC} = 1^{--}$. A unique property of e^+e^- physics with a storage ring is that the experiment is performed in the center of mass. This means that the total energy and momentum are known as well. A particular advantage over pp experiments is that the baryon number is zero, resulting in a considerable simplification of the final state. Thus the e^+e^- system is a particularly convenient probe to study photon-hadron coupling.

In the first two lectures we shall discuss the total cross section for hadron production and scale invariance as applied to e^+e^- annihilation. The second two lectures will concentrate on the narrow ψ resonances at 3.095 and 3.684 GeV; the general properties as well as specific decay modes will be discussed. Please note that I shall discuss mainly results from SLAC and DESY since Dr. Paoluzi will discuss results from Frascati. Also, where possible, reliance will be placed upon parallel lectures given by Drs. M. K. Gaillard, Söding, Nachtmann, and Appelquist to develop some subjects more thoroughly than these lectures allow. The bibliography is not intended to be exhaustive but rather should provide good background material, which in turn will have references for further study. Lastly, these lectures are frankly tutorial and are not intended to be a definitive review for specialists.

TOTAL CROSS SECTION

The photon propagator enters into very many forms of physics. The accuracy which is required for knowledge of the propagator sometimes is beyond the lowest order result. The fact that the photon interacts with the rest of the world can produce subtle or even dramatic effects on its propagator. The coupling between the photon's interactions and the effect on the propagator may be expressed through a dispersion relation.

$$D(s) = (1/s)/(1-\Pi(s)) . \tag{1}$$

Eq. (1) describes the photon propagator D as a function of s, the square of the photon's four-momentum. The factor 1/s describes the lowest order propagator, and the factor $1/(1-\Pi(s))$ sums all intermediate states; the imaginary part of D is related to the total cross section for $e^+e^- \to \gamma \to$ anything:

$$\mathrm{Im}(D) = -\sigma_T/(4\pi\alpha) , \tag{2}$$

or

$$\mathrm{Im}(\Pi) = -\frac{\alpha}{3} R_T(s) , \tag{3}$$

where

$$R_T(s) = \sigma_T(s)/\sigma_\ell(s) , \tag{4}$$

and

$$\sigma_\ell(s) = (4\pi\alpha^2/3s)/(1-\Pi(s)) . \tag{5}$$

The quantity σ_ℓ represents the total cross section for $e^+e^- \to \gamma \to \ell^+\ell^-$, i.e., producing a pair of point-like leptons whose mass is much less than $w \equiv \sqrt{s}$. A once-subtracted dispersion relation for Π may be written, taking advantage of the fact that $\Pi(0) = 0$.

$$\Pi(s) = \Pi(0) - \frac{\alpha s}{3\pi}\int \frac{R_T(s')\,ds'}{s'(s'-s-i\epsilon)} \tag{6}$$

We shall refer to the effects of Π on D as vacuum polarization corrections mainly in connection with the resonances, ψ.[10] The effects in principle are important to precision tests of Quantum Electrodynamics (QED).

Since the pair production of leptons is presumably well understood, a quantity of more direct interest than σ_T is σ_h, the total cross section for hadron production by e^+e^- annihilation. This is the simplest property of the hadronic system we can study, and likewise something which has the best chance of being understood theoretically. The most fundamental theoretical idea in $e^+e^- \rightarrow$ hadrons is that of scaling.[11] This means that σ_h should behave like 1/s for large s. Just what "large" means is not quantitatively addressed in most theoretical pictures; rather "large" means with respect to any characteristic energies or masses in the problem. Stated differently, the quantity R

$$R = \sigma_h/\sigma_\mu \tag{7}$$

$$\sigma_\mu = \frac{4\pi\alpha^2}{3s} \tag{8}$$

is expected to approach a constant for large s. The quantity σ_μ is the lowest order electromagnetic cross section for $e^+e^- \rightarrow \gamma \rightarrow \mu^+\mu^-$ (cf. Eq. (5)); this is a convenient reference cross section for the production of point particles. A compilation of data from Orsay, Frascati, CEA, and SLAC on σ_h is shown in Figs. 1 and 2. One can see the production of the vector mesons, ρ, ω, and ϕ, in the low energy region followed by a plateau of $R \sim 2.5$ extending up to $w \sim 3.5$ GeV. For the moment we shall ignore the two enormous peaks due to the narrow resonances! There is a broad enhancement at $w \sim 4.1$ GeV followed by another plateau where $R \sim 5$.

There are numerous approaches to the relation $R \rightarrow$ constant: The simplest (although deceptively so) is one of dimensional analysis. This argument says that when w is large compared to all masses which may enter, the only unit of length remaining is $s^{-\frac{1}{2}}$; thus the cross section must behave like s^{-1}. The simplicity of this argument should not be taken too seriously, since historically the

physics community was profoundly shocked by the experimental discovery that $R \sim 2$ about six years ago, because dimensionless form factors were expected to drastically reduce the cross section. The dimensional argument has been sharpened by Wilson's[12] operator product expansion indicating that form factors are not expected. Somewhat earlier some equally shocking results in deep inelastic electron scattering[13] forced new directions in theoretical thinking. These data made clear that there was some kind of scale invariance in photon-hadron interactions. One of the most appealing physical pictures which emerged is the parton model.

The parton model constructs hadrons out of point-like constituents. Except for the parton mass, this ansatz is manifestly a scale-invariant theory, for the dimensional argument is applicable. The identification of spin 1/2 quarks as partons is an extension which allows a very simple calculation of the constant R, viz.

$$R = \sum Q_i^2 \quad ; \tag{9}$$

that is to say, the total cross section for producing pairs of quarks is $Q^2\sigma_\mu$, where Q is the quark charge in units of the positron charge. (It is assumed that w is large compared to the quark mass.) In this picture the photon pair produces quarks with the characteristic point-like fermion cross section and the quarks eventually dress themselves as normal hadrons which can be observed. (We shall put aside the question of why the quarks or their end products do not reach the laboratory carrying their fractional quantum numbers.) An attractive feature of quark models is that they have a reason to exist besides simply explaining e^+e^- annihilation. Thus, for various reasons, different quark models have been constructed to solve various problems; as consequences they make predictions on R. The original Gell-Mann - Zweig model of

three quarks suffered a deficiency of requiring a new type of fermion statistics, where up to three fermions could occupy the same state; this had the result that a nucleon was made up of three fermions in a symmetric state. The introduction of a new SU(3) group of "color" has three times as many quarks with properties as before but with an extra quantum number of "color;" thus the statistical problem was solved. The original Gell-Mann - Zweig model predicts R = 2/3 (= 4/9 + 1/9 + 1/9), while the color model predicts R = 3(2/3)=2. (This result is not as obvious as it seems because the observed hadrons are supposed to be color singlets.) Another variant of the quark model involves the introduction of "charm". This extra type of quark having a charge of 2/3 was a useful means of allowing strangeness conserving weak neutral hadronic currents such as $\nu p \rightarrow \nu$ + hadrons but forbidding strangeness changing weak neutral currents such as $K^o \rightarrow \mu^+\mu^-$. As with color the known hadrons are supposed to be charm singlets. The color-with-charm scheme predicts R = 10/3. The Han-Nambu color scheme differs from the Gell-Mann color scheme by introducing more quarks but having integer rather than fractional charge. As a consequence this scheme predicts R = 4. Recently Harari[14] has proposed a model consisting of the usual three quarks plus a new antitriplet of "heavy" quarks having charges 2/3, 2/3, -1/3; all quarks also have the usual three "colors". In this model R = 2 below threshold for heavy quark production and R = 5 above threshold. (Harari's model was invented to describe the $e^+e^- \rightarrow$ hadrons data rather than for other reasons. Like the charm scheme, however, it permits strangeness conserving neutral currents and prohibits strangeness changing neutral currents.)

Returning to the data[7] shown in Fig. 2, it is clear that a scaling prediction of R = 2 is not a good description for the whole range of w > 2.0 GeV, although

it is not a bad description of the data for $2.0 < w < 3.5$ GeV. However, the enhancement at about 4.1 GeV clearly indicates that a new large mass scale is important, and $R \sim 2$ may or may not be fortuitous. There is a plateau of $R \sim 5$ which persists above that enhancement up to the maximum energy at which data are available, viz., $w = 7.4$ GeV. Perhaps there is still hope for a scale invariance. The 4.1 GeV enhancement is broad, $\sim$ 300 MeV, and thus is suggestive of normal hadronic resonances. Had the narrow ψ resonances[8,9] at 3095 and 3684 MeV not been found this broad enhancement would be merely a curiosity like the ρ'. Given the existence of the ψ's one must explore the possibility that all three are related, and that perhaps kinematics alone (phase space) has distinguished the 4.1 GeV enhancement from the ψ's in its width. Such would be the case if 4.1 GeV were just above the threshold for producing pairs of particles having a new quantum number such as charm. An important question is "How does the hadron production at the 4.1 GeV enhancement differ from hadron production nearby the enhancement?" At this time we have insufficient data to make a definitive statement; this question must await future data taking in order to study exclusive channels.

Much speculation has surrounded the 4.1 GeV enhancement trying to relate it to the two ψ resonances or trying to relate it to the increase in R from 2.5 to 5. Perhaps 4.1 GeV is the threshold for production of pairs of "charmed" particles; since charmed particles are expected to be long-lived, one might expect to find such states by studying various invariant mass combinations, especially those involving strange particles. Using our large block of data at $w = 4.8$ GeV we have searched[15] for such states: For lack of any convincing signal (see Fig. 3) we have set upper limits for inclusive production of charmed states. These limits are shown in Table I. The list of decay

modes does not, of course, exhaust all possibilities. In particular, modes with more than three particles become difficult to study by this technique because the combinatorial problem becomes formidable. (We cannot use time-of-flight particle identification because it severely limits the range of masses one can successfully search. The π-K separation is limited to momenta less than 700 MeV/c.) In addition, it may be that "charmed" mesons preferentially decay with a missing neutral either by hadronic or semileptonic decays.

It may be that some of the increase in R above 4 GeV is due to production of heavy leptons, which subsequently decay into multibody states. A single pair of such leptons would contribute less than 1 to R, however, since they should be produced with the same cross section as μ pairs. Thus it seems unlikely that this is a good explanation for the entire increase in R.

Finally, the opening of a new degree of freedom may be reflected in an increase in the charged multiplicity: Fig. 4 shows the corrected charged multiplicity as a function of w. It rises gradually from about 3.3 at w = 2.5 to about 4.9 at w = 7.4. This variation is consistent with many models of $e^+e^- \rightarrow$ hadrons. Incidentally, the charged multiplicity is similar to the annihilation part of $p\bar{p} \rightarrow$ pions.[16]

In the recent past the assumption of single photon exchange has been questioned[17] and a two-photon process proposed to explain the large value of R. Physically the process is shown in Fig. 5, where the e^+ and e^- each emit a photon; these in turn collide to produce hadrons. Even though such a process is higher order in α there are $\log^2$ terms which tend to compensate the extra power of α. Such a possibility considerably confuses the interpretation of an experiment on $e^+e^- \rightarrow$ hadrons because the final state electrons of the two-photon process will generally escape detection. Measurements made at

$w = 4.8$ GeV where a small fraction of those electrons are detected indicate that with the criteria used to define the hadronic events such a process does not seriously contaminate the measurement of $e^+e^- \rightarrow$ hadrons. In the next lecture we shall discuss evidence against this contamination at $w = 7.4$ GeV.

SPEAR DETECTOR

Let me digress for a while into some experimental details because some fundamental facts are required to put the experiments into perspective. As an illustrative case, SPEAR and the magnetic detector in use there will be discussed.

An artist's view of the detector is shown in Fig. 6. The detector consists of a large solenoidal magnet whose field is parallel to the e^+e^- beam direction. The interaction region is surrounded by a set of cylindrical spark chambers disposed at radii between 65 and 135 cm from the interaction point. These spark chambers allow track reconstruction over the range of polar angle $-0.7 < \cos(\theta) < 0.7$. Outside the spark chambers is a set of scintillation counters used as part of the trigger as well as for measuring time of flight for final state particles. In addition, but outside the magnet coil, there is a set of "shower" counters which also are a part of the trigger; these counters are sensitive to minimum ionizing particles but are also useful for identification of electrons or photons. These counters subtend the polar angle range $-0.65 < \cos(\theta) < 0.65$.

The most important lesson to be learned from this description of the apparatus is that the event selection is biased: First, the trigger requires at least two charged particles having momenta > 200 MeV/c to record the event at all. This requirement was necessary in order to reduce the background rates to tolerable levels. Thus the apparatus is insensitive to final states consisting entirely of neutral particles; this is not so serious a shortcoming as it appears at first sight because a state of all π^0's is excluded by charge conjugation if the one photon approximation is applicable. Secondly, the trigger only covers about 65% of the total solid angle. Thirdly, event identification

can also introduce bias and thus the need for corrections. The identification of an e^+e^- pair in the final state uses the energy deposited in the shower counters and the topology of a two-body final state, viz., the two particles must be nearly collinear. A pair of muons in the final state differs from an electron pair only by virtue of the energy deposited in the shower counters. (Thus we cannot exclude the possibility of two-body hadronic final states being included in this sample. Such a contamination, however, is expected to be very small. During part of the running the information from the muon chambers was available and more direct muon identification was possible.) The hadron sample must exclude these QED processes; a hadron event is defined as one having three or more charged particles or, if there be two, their momenta must exceed 300 MeV/c and the plane formed by them must not contain the beam line. (The momentum cut reduces the background due to $\gamma\gamma$ reactions and the coplanarity cut excludes $e^+e^- \rightarrow e^+e^- \gamma$, which produces acollinear e pairs.) Thus in the end one must compensate for the bias introduced by the trigger requirement and the event selection. This estimation of event losses is always model-dependent to some extent, and the larger the correction, the larger the uncertainty in the final answer due to this model-dependence. One must perform as many checks as possible on the model to assure that it accurately reflects the data. The net uncertainty is about 10 to 15% for the overall detection efficiency, which itself ranges from 0.4 to 0.7 as w ranges from 2.4 to 7.4 GeV.

INCLUSIVE SPECTRA AND SCALING

Let us now turn to the subject of single particle inclusive spectra,

$$e^+e^- \rightarrow h + \text{anything} \tag{10}$$

where "h" is any hadron. If "h" is an antiproton this reaction is the complete analog of the deep inelastic electron scattering experiments in the annihilation region rather than the scattering region. Assuming the one-photon exchange approximation and that the beams are unpolarized we can write the most general form for the cross section for reaction (10).

$$\frac{d\sigma}{dx d\Omega} = \frac{\alpha^2\beta}{4s}\left[W_1(x,s)(1+\cos^2\theta) + W_0(x,s)(1-\cos^2\theta)\right] \tag{11}$$

where $x = 2p_h \cdot q/s = 2E_h/w$,

$\beta = p_h/E_h$,

and θ is the angle between the outgoing hadron and the incident positron, q is the four-momentum of the photon, and p_h and E_h are respectively the momentum and energy of the detected hadron; β is the velocity of the hadron. This particular decomposition is convenient because all possible physics obtainable from such a set of measurements about the hadronic system is contained in the two structure functions W_1 and W_0, which respectively describe helicity 1 and helicity 0 final states. For deep inelastic electron scattering a completely analogous decomposition of the cross section into two structure functions exists, where s is replaced by $-q^2$ in the definition of x, and E_h corresponds to the target proton, rather than an exiting particle. The major result of deep inelastic electron scattering was that the structure functions are really only functions of x rather than x and s. This is the manifestation of scaling. The similarity between $e^-p \rightarrow e^-$ + anything and $e^+e^- \rightarrow h$ + anything

is schematized in Fig. 7. The two reactions are related by crossing. (Beware, this is not to say that the structure functions are necessarily simply related.) The fundamental idea that the structure functions in both the space-like and time-like region are functions only of x is appealing, if not rigorously established theoretically. Carrying the same ideas to annihilation, the hypothesis that W_1 and W_0 depend only on x means that s $d\sigma/dx$ depends only on x, in the limit $\beta \to 1$. Fig. 8 shows data[18] from SPEAR at w = 3.0, 3.8, and 4.8 GeV for s $d\sigma/dx$. (Higher energy data have not yet been adequately analyzed for this test.) It is clear that as a whole the data disagree strongly with the scaling hypothesis. Note, however, that the data from the three energies overlap well for $x > 0.5$, i.e., scaling works at high x. That scaling fails in this plot should be no surprise, having seen that σ_h itself does not exhibit the expected scaling behavior: Recall that

$$\int_0^1 \frac{d\sigma}{dx}(s)\,dx = \langle N_{ch} \rangle \sigma_h \qquad (12)$$

(each charged particle of an event contributes to the plot of s $d\sigma/dx$). If R is constant (i.e., s σ_h is constant) and s $d\sigma/dx$ is independent of s, then the integral of s $d\sigma/dx$ determines $\langle N_{ch} \rangle$. (Note that while formally the lower limit of integration is x = 0, in reality masses prevent particles from reaching x = 0; thus in the scaling model the s-dependence of $\langle N_{ch} \rangle$ is allowed even though s $d\sigma/dx$ is independent of s. Furthermore some s-dependence is expected in s $d\sigma/dx$ in the region where β is not near one.) Since R changes by a factor of 2 over the range $3.0 < w < 4.8$ GeV and $\langle N_{ch} \rangle$ changes only slightly, we must conclude that s $d\sigma/dx$ should not scale. Conversely, for $w > 4.8$ GeV we should not be surprised to see scaling obtain in s $d\sigma/dx$ since R is roughly constant and $\langle N_{ch} \rangle$ is changing slowly. We must await the data to confirm this suggestion.

Another interesting way to look at the inclusive spectra is to plot $d\sigma/d(\text{invariant phase space}) = d\sigma/(d^3p/E)$. Fig. 9 shows the data at 3.0, 3.8, and 4.8 GeV. Curiously, this plot appears to be universal curve, independent of s. Superposed upon the SPEAR data are lines representing the shape of the invariant cross section for $pp \rightarrow \pi$ + anything at 90^o c.m. from Cronin et al.[19] at 200 GeV. It is curious that the slope of the pp data is so similar to the e^+e^- data. Whether the relation will persist at higher e^+e^- energies will be interesting because such universality is ideally suited to statistical models. Except for the singular case $s\, d\sigma/dx = x^{-3}$ it is not possible for both $s\, d\sigma/dx$ and $d\sigma/(d^3p/E)$ to be independent of s. It is difficult to take the special case $s\, d\sigma/dx = x^{-3}$ too seriously because it predicts a relatively large yield at $x = 1$. This would conflict with deep inelastic scattering data which span the region $x > 1$ but approach zero as $(x-1)^p$, where p is a power. While it is true that as a general case one cannot analytically continue the structure functions from the space-like region to the time-like region, various specific models have been made to estimate the time-like structure functions from the space-like structure functions. In all cases there is continuity across $x = 1$. The scaling of the invariant cross section and of the structure functions are quite different descriptions of nature. Thus at least one of these two kinds of scale invariance will probably fail at higher energy.

The relative yields of particles is another interesting number for various models. Fig. 10 shows the invariant cross section for π, K, and p production at 4.8 GeV. It is interesting that all three kinds of particles appear to lie on a universal curve. That is to say that the number of particles produced at any given energy (not momentum) is roughly independent of the type of particle. A different question is how the relative fraction of charged particles which are

kaons varies with s. The suggestion of the opening of "charmed" channels above 4.1 GeV also suggests that there be a larger fraction of kaons above that threshold. Figure 11 shows that fraction as a function of momentum for w = 3.0 and 4.8 GeV. Clearly there is no dramatic change in the spectrum of events having kaons of momentum less than 700 MeV/c as the energy crosses this threshold. (Experimentally the identification of kaons at higher momenta becomes prohibitively difficult.) We shall return to discuss the kaon yield at the resonances later. The featureless behavior of the nonresonant K production presents a challenge to models of the step in R.

Let us return to the discussion of the structure functions of Eq. (11). Since those two functions contain all possible physics obtainable from the single particle inclusive experiment, we should like to separate the two. In principle this is possible because of the different angular dependence: W_1 goes with $1 + \cos^2(\theta)$ and W_0 goes with $1 - \cos^2(\theta)$. In practice this is not easy with finite statistical samples in a limited angular coverage detector. One can ask if any additional information may be obtained if the e^+ and e^- beams are polarized. The answer is yes, but for a surprising reason: There is no new physical information available but the gain is instrumental. To see this let me describe an elegant theorem due to J. D. Bjorken: Under the assumption of the single photon intermediate state the cross section for any specified final state f, no matter how complicated, for completely polarized beams may be calculated analytically from the unpolarized cross section. (Thus no new physics!) The algorithm is simple: Suppose the e^+ and e^- beams travel along the z-axis in the unpolarized case and one knows the analytical form for the cross section to find state f, $\sigma_f(z)$. Then the case where the beams are completely polarized vertically, along the y-axis, may be

calculated by adding to $\sigma_f(z)$ the cross section when the beam direction is along the x-axis and subtracting the cross section for y-axis beam direction:

$$\sigma_f(\text{polarized}) = \sigma_f(z) + \sigma_f(x) - \sigma_f(y) . \tag{13}$$

The result for an arbitrary polarization for each beam P is now easily obtained

$$\sigma_f(P) = (1-P^2)\,\sigma_f(\text{unpolarized}) + P^2\sigma_f(\text{polarized}) . \tag{14}$$

As an example, applying Eq. (13) and (14) to (11), we obtain

$$\frac{d\sigma}{dx d\Omega} = \frac{\alpha^2\beta}{4s}\left[W_1(1+\cos^2\theta)+W_0(1-\cos^2\theta)+P^2(W_1-W_0)\sin^2\theta\cos 2\phi\right] \tag{15}$$

Thus by measuring the azimuthal distribution and the beam polarization, one measures the difference between W_1 and W_0. (Stated differently, this measurement determines the ratio $(W_1 - W_0)/(W_1 + W_0)$.) As a result, one can accurately calculate the entire $\cos\theta$ distribution from this knowledge even though one has limited $\cos\theta$ coverage. Some very recent results from SPEAR are shown in Fig. 12, where the azimuthal distribution of all hadrons having $x > 0.3$ are plotted at two different beam energies. The data taken at 6.18 GeV were taken on a spin depolarizing resonance where no polarization effects are expected, while the data at 7.38 GeV were taken where normal beam polarization could take place. The azimuthal non-uniformity in the latter case is quite striking and promises to be a very powerful tool in measuring angular distributions and separating form factors. It might also be noted that the amount of non-uniformity of the azimuthal distribution is quite compatible with the expected beam polarization. Furthermore, the observation of polarization effects speaks strongly in favor of the single photon intermediate state hypothesis, at least for those high energy prongs.

It is perhaps worthwhile to briefly discuss the process of beam polarization, since such effects are important. The emission of synchrotron radiation by the electron beams, in the absence of other depolarization effects, results in polarization of the beams parallel to the magnetic guide field.[20] The electrons and positrons are polarized in opposite directions. Although the question of what energies should produce beam polarization is complex, it is easy to see why w = 6.18 GeV should not have beam polarization. Recall that the spin of an electron precesses with respect to the orbit $\nu = \frac{\Delta\phi \text{ spin}}{\Delta\phi \text{ orbit}} = (E/m_e)(g-2)/2$ times the orbit frequency. Thus if the orbit frequency and the spin precession frequency are commensurate, slight field perturbations act coherently upon the spin resulting in depolarization. The width of such a resonance is also complicated, but it is at least as wide as the beam resolution, $\sim 0.1\%$. In principle, one could imagine an ultimate calibration of the storage ring against g - 2 of the electron.

ψ RESONANCES (GENERAL)

The world of e^+e^- physics took a sharp turn with the discovery of the two resonances, ψ (3095)[8,21] and ψ (3684).[9] Figures 13 and 14 summarize the cross sections for $e^+e^- \rightarrow$ hadrons, $\mu^+\mu^-$, and e^+e^- near the two resonances. Important qualitative features of Fig. 13 and 14 are the magnitudes of the hadronic cross section compared to the baseline (which was itself "yesterday's" excitement), and widths which are consistent with the energy resolution alone. The effect in both the lepton channels is dramatic for the ψ (3095) but much less so for the ψ (3684). This means that the branching ratio of ψ (3684) to leptons is substantially smaller than for ψ (3095). Even so, the effect on the lepton rate compared to the QED rate is quite significant; thus the vacuum polarization effects discussed in the first lecture become large at the resonances (assuming no direct lepton coupling). The skewed shape of the curves is mostly due to radiative effects which spread the beam energy asymmetrically. As we shall soon see, the widths of these resonances, respectively 69 and 228 keV, are far narrower than the energy resolution of the storage ring, which is of the order of 1.1 to 1.5 MeV.[22] The high masses alone are exciting, but the great excitement stems from the very small widths. The widths suggest that either the decays are not hadronic, or some new quantum number dramatically retards the usual hadronic decays. Generally speaking, hadronic decay widths are of the order of 10 to 100 MeV. A notable exception to this guide is $\phi \rightarrow K^+K^-$, but this mode is severely inhibited by phase space. First-order electromagnetic decays have widths of the order of 0.1 to 1 MeV, and second-order electromagnetic widths are of the order of a few keV. As we shall see, the ψ's share the quantum numbers of the photon $J^{PC} = 1^{--}$, but photon coupling alone through second-order electromagnetic effects (i.e., vacuum polarization) cannot account for a large fraction of hadronic final states.

As soon as the resonances were discovered the charm and color models were actively reexamined,[23-25] since they are logical possibilities for a new quantum number preventing decays to ordinary hadrons. Noting that the required coupling to e^+e^- was of the order of magnitude for weak interactions, it was also suggested that the weak vector boson had been found (in spite of the rather low mass compared to expectations). Now, as much more information is available, the charm model shows much more promise than the others, but it too has difficulties.

In the charm model the two resonances are viewed as pure charmed quark pairs, $c\bar{c}$, and the decay to hadrons should be strong but inhibited by Zweig's rule. This empirical rule says that two ends of the same quark line cannot belong to the same hadron. This means that no disconnected graphs are allowed. The decay of the ϕ to hadrons proceeds mainly through $K\bar{K}$ states because ϕ consists of a nearly pure $s\bar{s}$ state; the decay rate would be much less if the strange particle states were not kinematically accessible. Thus for the ψ's the model supposes that these resonances are below threshold for charmed meson pair production and the 4.1 GeV enhancement fits into the same scheme if it is above the threshold for charmed meson pairs. The charm model predicts a large number of possible $c\bar{c}$ states, however not all are expected to be narrow, and not all are natural parity vector states.

The study of the general properties of the resonances such as the decay widths, spin, and parity is a nice exercise in quantum mechanics.[26] Let us begin by recalling some nuclear physics. A general description for the cross section for $e^+e^- \rightarrow \psi \rightarrow f$, where f is any final state, is the Breit-Wigner formula,

$$\sigma_f(w) = \frac{\pi(2J+1)}{s} \frac{\Gamma_e \Gamma_f}{(w-m)^2 + \Gamma^2/4} \tag{16}$$

where J is the spin of the resonance, m is its mass, and Γ is its total width. The quantities Γ_e and Γ_f are respectively the partial widths of the resonance to electron pairs and the final state f. This formula is mainly an expression of unitarity and time reversal invariance. Because the experimental resolution is large compared to Γ, $\sigma_f(w)$ behaves nearly like a delta function and the experiment is mainly sensitive only to the integral of $\sigma_f(w)$

$$\int \sigma_f(w)\, dw = \frac{2\pi^2}{m^2} \frac{\Gamma_e \Gamma_f}{\Gamma} \,. \tag{17}$$

We shall see that the ψ resonances interfere with photons and therefore have $J^{PC} = 1^{--}$; one can then fit the excitation curves of Figs. 13 and 14 to obtain Γ_e, Γ_μ, and Γ_h for the electron, muon, and hadron partial widths. To do this we must also assume that the total width $\Gamma = \Gamma_e + \Gamma_\mu + \Gamma_h$. Intuitively one can see how to extract Γ_e and the branching ratios into hadrons, muons, and electrons simply by comparing the integrated cross sections for the three channels. The sum of the three directly determines Γ_e alone. Then the ratios of the three channel integrals to the sum determines the branching ratios. (Naturally to obtain the integrals one must subtract the nonresonant backgrounds.) Statistically one can do better by making a simultaneous fit to the three distributions, fitting m, Γ_e, Γ_μ, Γ_h, the background hadron cross section, and the beam resolution. (The QED cross sections are fixed.) The fitting must take into account the interference of the Breit-Wigner amplitude with the nonresonant amplitude. For the lepton channels this process is well understood; the relative phases can be seen by use of the dispersion integrals discussed in the first lecture if there is no direct lepton-ψ coupling, but only via a photon;

the phases, however, are more general than this argument indicates. A way to see the phases is to refer to Fig. 15, which is an Argand plot for the sum of the QED amplitude and the Breit-Wigner resonance amplitude. The QED amplitude is real and negative; μ-e universality plus causality fix the direction of travel around the resonance. Thus the relative phases of the two amplitudes are fixed, and the sign of interference effects is unambiguously fixed. The hadron channel is not clear because direct hadron-ψ coupling will be shown to be important in channels which do not significantly couple to the photon; thus there are channels which may contribute incoherently; fortunately the final answer is almost independent of such interference in the hadron channel. (The mechanics of the fitting also involves a number of details regarding the intrinsic beam resolution and radiative effects; these details do not interest us here.) The results of such fits to data for both resonances are shown in Table II.

It is interesting to compare some of the properties of the well-known vector mesons (as of a year ago) with the two new ones which have been added. Table III shows the mass, the total width, the partial width to electrons, and the coupling constant f, where f is related to Γ_e by

$$\Gamma_e = \frac{4\pi\alpha^2}{3}\frac{m}{f^2} \tag{18}$$

In addition to the $\psi(3095)$ and $\psi(3684)$ the 4.1 GeV enhancement has also been included, although the case for its being a vector meson is not proven. (Of course the suspicion is strong since we believe that it results from single photon e^+e^- annihilation.) Even though the total widths span over three orders of magnitude, their partial widths to electrons do not span a factor of 10. The SU(3) prediction for the relative magnitudes of the coupling constants for ρ,

ω, and ϕ is known to work fairly well, viz., $f^{-2}\rho : f^{-2}\omega : f^{-2}\phi = 9 : 1 : 2$. The extension of this prediction to a $c\bar{c}$ model says[23] $f^{-2}\rho : f^{-2}\omega : f^{-2}\phi : f^{-2}\psi(3095) = 9 : 1 : 2 : 8$. In the color model[24] the $\psi(3684)$ is also predicted and $f^{-2}\rho : f^{-2}\omega : f^{-2}\phi : f^{-2}\psi(3095) : f^{-2}\psi(3684) = 9 : 1 : 2 : 8 : 4$. As can be seen from the table the relative magnitude of $\psi(3095)$ and $\psi(3684)$ is roughly correct, but the coupling of the two does not match well with the other vector mesons. Perhaps one should not be too concerned by this failure because the mass differences are so large. It has been pointed out[27] that this SU(3) relation works better for Γ_e than for $(f^2/4\pi)^{-1}$; perhaps this is the preferred comparison.

It is easy to see that the decay of the resonances to hadrons cannot all be due to vacuum polarization effects. If this were so, and there are no direct couplings of μ pairs to the resonance, then the enhancement of the μ pair rate over QED at the resonance is a direct measurement of those second order electromagnetic effects; defining $B_h = \Gamma_h/\Gamma$, etc.,

$$B_h(\text{resonant}) = B_\mu(\text{resonant})\Gamma_h(\text{nonresonant})/\Gamma_\mu(\text{nonresonant}) \quad . \tag{19}$$

For $\psi(3095)$ this relation predicts $B_h = 0.17 \pm 0.03$ while the branching ratio is 0.86 ± 0.02. For the $\psi(3684)$ the numbers are $B_h = 0.029 \pm 0.004$ vs. 0.981 ± 0.003. Clearly the vacuum polarization enhancement is only a small part of the total width and therefore the decays to hadrons must be direct.

One clear prediction of the charm model is that besides the two low-lying states of relative angular momentum $L = 0, 2$ there are other vector states involving radial excitations. This argument notwithstanding, it is an obvious experiment to see if there be any other narrow resonances which couple to e^+e^-. Such experiments were carried out at SLAC[28] and Frascati,[29] but no new narrow resonances have been found. Figure 16 shows data from the SLAC

experiment which covered the range $3.2 < w < 5.9$ GeV. Later data, not shown, extended this search up to 7.6 GeV. Table IV shows the upper limits which are placed on the integrated cross sections from the SLAC data.

In the analysis of Γ_e, etc., we have assumed spin 1 for the ψ's, promising to justify this assumption. Before doing so let us briefly examine the implications of $J \neq 1$. The "law of least amazement" says that e^+e^- must couple to one photon and thus the ψ's must share the quantum numbers of the photon. Another possibility is that the ψ's are the result of two photon annihilation. This is not very attractive and the value of Γ_e is the right order of magnitude for a single photon coupling like the vector mesons. Perhaps e^+e^- could couple through weak interactions, but not through the usual V-A mixture or for that matter, any mixture of V and A. The hypothesis of weak interaction coupling is attractive since the magnitude of Γ_e of few keV is about right, but we shall see that there is little else to support this conjecture. The last possibility is the discovery of a new force in elementary particle physics.

The establishment of the J^{PC} assignment for the two resonances rests upon study of the lepton channels. Primary evidence comes from interference between the resonant amplitude and the QED amplitude. For the purpose of minimizing systematic errors due to normalization, the ratio of μ pair yield to e pair yield is shown in Fig. 17 for each resonance. Interference effects in the e^+e^- channel are small compared to the $\mu^+\mu^-$ channel because the e^+e^- QED amplitude is dominated by space-like photon exchange. Likewise the sign of the interference in the electron channel integrated over the detector is opposite that of the μ pairs. Figure 17 shows fits with and without interference effects included: For both resonances the interference fits are quite acceptable while the no interference fits are incompatible by 2.7 and 4.9 standard deviations,

respectively. Assuming conservation of P and C, the observation of this interference implies that the resonances must have the same quantum numbers as the photon, viz. $J^{PC} = 1^{--}$. (Strictly speaking the conclusion requires more justification because the detector does not cover the full solid angle; thus different J states are not orthogonal. Spin 0 can show no interference, but spins 2 and 3 can show interference, but the sign is opposite that of J = 1 when integrated over $|\cos\theta| < 0.6$. Spins higher than 3 will show no significant interference. The symmetries of the detector make the orthogonality of different P and C states persist in spite of limited solid angle.) Confirmatory evidence for the spin assignment comes from the angular distributions of the leptonic decays of the resonance. Data from SLAC are shown in Figs. 18 and 19. A J = 1 state is expected to result in an angular distribution of $1 + \cos^2(\theta)$; the data from this experiment and from DESY[30] are consistent with this hypothesis, although not compelling. (Technically, a spin 2 state can exactly reproduce $1 + \cos^2(\theta)$ and a spin 3 state can well approximate that distribution over the range of $\cos\theta$ measured if both helicity states 0 and 1 are available. Conservation of CP,[31] however, forbids helicity 0 states for J = 2.) Having established the existence of an interference effect one can use the angular distributions to turn the argument the other way and obtain a test of the relative sign of the μ-e coupling to the resonances. The observation of interference with QED implies that a major part of the lepton coupling must be through helicity one states. Such states have angular distributions for spins 2 and 3 which are completely incompatible with the observations. Thus we can exclude the possibilities of J = 2 or 3 with opposite sign e-ψ and μ-ψ coupling. The assignment J = 1 immediately excludes the suggestion that the ψ's are Higgs scalars.

Additional information is available from DESY, where the channel $e^+e^- \rightarrow \gamma\gamma$ was sought;[32] they found an upper limit of 3.4×10^{-3} for the branching ratio in this mode. This decay mode is strictly forbidden for a spin 1 state. To see this, observe that a two real photon final state can only have helicities -2, 0, +2, while a spin 1 state can only contribute to helicity states -1, 0, +1. The only overlap is a helicity = 0 state; this state, however, is antisymmetric for J = 1, which violates the requirement of Bose-Einstein statistics.

The asymmetries of the angular distributions shown in Fig. 20 allow tests of parity conservation. An admixture of positive parity will interfere with the negative parity amplitude resulting in an angular asymmetry at the resonance. For both resonances the asymmetries are consistent with zero throughout. (Radiative corrections imply that an asymmetry of the order of 2% should be observed; the data have not been corrected for this effect.) Thus we conclude that the resonances are rather pure states of negative parity. The purity of the parity of the ψ's strongly argues against the suggestion that they be weak vector bosons, since those would be expected to have V-A coupling, which is the strongest possible parity violation.

An interesting question is whether the decay of the ψ has a larger number of K's than the nonresonant hadron production. Figure 21 shows the fraction of charged particles identified by time of flight which are π, K, and p, respectively, as a function of momentum. This figure should be compared with Fig. 11 for the equivalent plot near the resonance. There is no dramatic difference between $\psi(3095)$ and w = 3.0 GeV, although there is perhaps a small excess at w = 3.0 compared to $\psi(3095)$. The equivalent plot for $\psi(3684)$ is not given because it would be heavily contaminated by the large fraction of $\psi(3684) \rightarrow \psi(3095)$ + anything decays.

ψ RESONANCES (SPECIFIC CHANNELS)

As with all studies of resonances the details of the decay modes which are seen and which are not seen give valuable information. Such a study turned up some surprising differences between the $\psi(3095)$ and the $\psi(3684)$.

Let us begin with the decay modes of the $\psi(3095)$. This has proven to be a rich field where many channels have been isolated, allowing determination of the G parity and exploration of the SU(3) structure. The most obvious channels to study are all pion states; these are easily treated and are copious. Clear signals are seen in the states of 3, 4, 5, 6, 7, and 9 pions, while DESY[33] has presented an upper limit for 2 pions. Table V summarizes the branching ratios of these modes. Clearly those states having an odd number of pions are favored. What is not immediately clear is just how strongly they are favored. Indeed the branching ratios into an even number of pions can be completely accounted for by second order electromagnetic effects. To see this it is convenient to study the ratios of the hadron cross section to the measured μ pair cross section both on and off the resonance; these are analogous to R_T of Eq. (4). Define

$$\alpha = R_{on}/R_{off} \tag{20}$$

as the ratio of these two ratios respectively on the resonance and off at w = 3.0 GeV; this ratio should be unity for any decay mode proceeding entirely through electromagnetic decay; conversely α will exceed unity for direct decays to hadrons. Figure 22 shows such a comparison for 3, 4,...,7 pion states. Clearly the odd number of pion states are incompatible with purely electromagnetic decays, while the even pion states are well explained by such vacuum polarization effects. Off resonance the odd number of pion states are scarce, resulting in the error bars which go up off the page; the limits shown are

conservative. Figure 23 shows missing mass spectra for the hypothesis of four charged pions seen at w = 3.0 GeV and at the $\psi(3095)$. The signal in $2\pi^+2\pi^-\pi^o$ for the resonance is dramatic, but there is no clear signal at w = 3.0 GeV. The purity of the G parity selection is striking and argues that the $\psi(3095)$ decay is hadronic, since strong interactions are the only ones known to conserve G parity. We can now conclude that the G parity of the $\psi(3095)$ must be -1. This fact implies that the isospin of $\psi(3095)$ must be even, since $G = C(-1)^I$.

We have three pieces of evidence indicating that I = 0:

(1) The three pion state is dominantly $\rho\pi$. Figure 24 shows the Dalitz plot for the three pion state; there are three distinct bands corresponding to ρ^+, ρ^-, and ρ^o. The branching ratios into the three states are roughly equal, and $B(\rho^o\pi^o)/(B(\rho^+\pi^-) + B(\rho^-\pi^+)) = 0.59 \pm 0.17$. An isospin zero state should produce the relative branching ratios $B(\rho^o\pi^o) : B(\rho^+\pi^-) : B(\rho^-\pi^+)$ of 1 : 1 : 1 while an isospin 2 state should have 4 : 1 : 1. Thus I = 0 is clearly favored.

(2) Both DESY[33] and SPEAR have observed $\psi(3095) \rightarrow p\bar{p}$. Figure 25 shows the reconstructed mass of each of a pair of particles obtained from kinematics alone; a clear proton signal is seen. By comparison with data taken away from the resonance (at w = 3.0 GeV where no events are observed) we know that these decays are not due to a vacuum polarization enhancement. Since a $p\bar{p}$ state can only be I = 0 or 1, we must select I = 0.

(3) We have also seen $\psi(3095) \rightarrow \Lambda\bar{\Lambda}$. Figure 26 shows the momentum of the Λ vs. that of the $\bar{\Lambda}$; there is a clear cluster at 1.07 GeV/c, which is correct for Λ pair production. Such an observation selects I = 0.

Returning to Fig. 22 we observe a bonus. We can turn the argument around and say that since the 4 and 6 pion events are really consistent with vacuum

polarization enhancement, then this is evidence that the lepton pairs must couple through a photon rather than having some direct interaction with the ψ.

Since the question of radiative decays is so crucial to the color model it is important that the observation of $n(\pi^+\pi^-)\pi^o$ states be clearly distinguished from $n(\pi^+\pi^-)\gamma$ states. The technique used distinguishes the π^o only by missing mass and is subject to some uncertainty. Assuming the π^o hypothesis, however, gives a clear ρ signal in the three pion state. (Cf. Table V.) Likewise clear ρ and ω signals are seen in the five pion state; thus it seems unlikely that the π^o could be a γ in disguise.

The study of other decay modes provides additional information on the SU(3) structure of the $\psi(3095)$. In particular a $c\bar{c}$ state would be a SU(3) singlet and should not decay into a pair of pseudoscalar mesons. DESY[33] has established an upper limit of the branching ratios $B(\pi^+\pi^-) < 3.2 \times 10^{-4}$ and $B(K^+K^-) < 5.8 \times 10^{-4}$ (using the SPEAR value of $B(\mu^+\mu^-)$). SPEAR data set an upper limit on $B(K_S K_L) < 2 \times 10^{-4}$. Similar arguments based on an extended charge conjugation[34] say that $K^*\bar{K}^*$ is forbidden; limits have been set which are significantly below the observed rates for $K\bar{K}^*$ states, which are allowed, and should offer a characteristic scale against which to compare the upper limits. Another prediction is that an SU(3) singlet should have the same decay rate into $\rho^o\pi^o$ as $K^o\bar{K}^{*o}(892)$. This prediction fails by about a factor of three so the picture is not perfect.

The search for radiative decays can give some evidence for nearby states of even C. DESY has established a limit on $\psi(3095) \rightarrow \gamma X^o$, where the mass of the X^o exceeds 2.6 GeV, viz., $B(\psi \rightarrow \gamma X^o)B(X^o \rightarrow \gamma\gamma) < 0.02$ (using the SLAC value of B(ee)).

An obvious question is "How large a fraction of the ψ decays can be clearly reconstructed as exclusive channels?" From Table V we have 14% for the leptonic decays, 17% for the second order electromagnetic hadronic states, 10% for direct pion decays, and about 3% for miscellaneous other states. Isospin arguments suggest[34] the multipion decays involving more than one neutral are 15%. This total is about 60%. The rest must consist of complicated states which do not satisfy the selection criteria our simple minds can make.[35]

The decays of the $\psi(3684)$ have proven to be quite different in character from the $\psi(3095)$. Table VI shows the known modes. Apart from the leptonic mode, which has already been discussed, and an expected vacuum polarization enhancement, the only measured decay of the $\psi(3684)$ involves a cascade to the $\psi(3095)$. Fig. 27 shows a pretty example of $\psi(3684) \rightarrow \psi(3095)\, \pi^+\pi^-$, where the $\psi(3095)$ decays into two electrons. The mode $\psi(3684) \rightarrow \psi(3095)\, \pi^+\pi^-$ suggests that the $\psi(3684)$ should also have negative G parity. The total cascade rate, $\psi(3684) \rightarrow \psi(3095)$ + anything suggests that the $\psi(3684)$ is I = 0 because a dipion state of I = 0 should have twice the rate for $\pi^+\pi^-$ as $\pi^o\pi^o$ (which are not directly observed in our experiment). The small amount not so accounted may be explained by the observation of $\psi(3684) \rightarrow \psi(3095)\eta$, which again confirms I = 0. Hilger et al.[36] report a value for $B(\psi(3684) \rightarrow \psi(3095)\pi^o\pi^o)$ which is in agreement.

I had intended to discuss limits on monoenergetic gamma ray production as tests for intermediate states as predicted in the charm model. As we have learned two days ago from Professor Söding's announcement of the discovery at DESY[37] of an intermediate state having γ coupling to both $\psi(3684)$ and $\psi(3095)$, any discussion of upper limits on such processes is hopelessly obsolete. The study of these states will be a rapidly expanding field.[38]

It is interesting to see how different the $\psi(3095)$ and $\psi(3684)$ are in their exclusive channel decay. As we have seen, the three pion mode of $\psi(3095)$ is a strong signal and it is dominated by $\rho\pi$. Figure 28 shows the distribution of total energy reconstructed for two prong events under the hypothesis that the missing momentum is taken by a π^o. For the $\psi(3095)$ there is a clear peak at the resonance energy where such events should appear. The remainder of the events represent more missing particles. For the $\psi(3684)$, however, the character is quite different. There is hardly a suggestion of a peak at the resonance energy: the $\rho\pi$ branching ratio is dramatically smaller than for $\psi(3095)$, with an upper limit of 0.1%.

The four prong events are equally dramatic in this disparity. Figure 29 shows the missing momentum vs. the observed energy assuming that the four charged particles having total charge = 0 are pions. For $\psi(3095)$ there are three clear clusters along the line of zero missing momentum; these correspond to $2\pi^+2\pi^-$, and $\pi^+\pi^-K^+K^-$ and $\pi^+\pi^-p\bar{p}$, where in the latter cases the wrong mass hypothesis causes the energy to be less than the ψ mass. There is a clear band extending up from the $2\pi^+2\pi^-$ cluster corresponding to $2\pi^+2\pi^-\pi^o$. The decay of $\psi(3684)$ is quite different. (Cf. Fig. 29 b-d.) In fact, once the $\psi(3684) \rightarrow \psi(3095)\,\pi^+\pi^-$ cascade decays are removed there is hardly any clustering anywhere. Understanding the difference between $\psi(3095)$ and $\psi(3684)$ decays may be a valuable step in understanding their nature.

The above arguments for the $\psi(3684)$ apply equally well to modes if a π^o is replaced by a γ, since the kinematics are nearly the same. Thus these results plus the limits on $\pi^o\gamma$ or $\eta\gamma$ decays from DESY[39] place severe constraints upon color models, which strongly favor radiative decays.

As with the $\psi(3095)$ one can ask what fraction of the total width we can

clearly reconstruct for the $\psi(3684)$. The leptonic modes are 2%, vacuum polarization enhancement is 3% and the cascade decay is 57%. Again one reaches about 60% for the total.[40] The character of what we do see, however, is quite different. Besides the cascade the only normal hadronic decays seen are compatible with just vacuum polarization enhancement. Thus there may be some new dynamical principle yet to be discovered which will explain this anomaly.

CONCLUSION

Our understanding of e^+e^- annihilation has grown dramatically in the past two years although many new questions have also arisen. We have seen that scaling in the total hadronic cross section has gone through two stages: There is a plateau between 2.0 and 3.5 GeV where the ideas of scaling seem to work, but a new scale of energy becomes important at around 4 GeV. Above 5 GeV there may be a new scaling region which persists up to 7.4 GeV.

The two narrow resonances are now well-established vector mesons but their widths are unusually small, while their partial widths to leptons are comparable to the other vector mesons. The absence of first order radiative decays is a serious problem for the color model. The charm model has several successes, viz., the SU(3) related predictions of $I = 0$, $G = -1$, and SU(3) singlet structure. On the other hand, the absence of other narrow states is puzzling; however, the announcement of states between $\psi(3684)$ and $\psi(3095)$ having single γ transitions adds considerably to the charm picture. The absence of charmed states above the threshold expected for pair production may be a fundamental problem for the charm model, but limits so far established are not decisive.

ACKNOWLEDGEMENTS

Much of the experimental work reported here is due to the SLAC-LBL Collaboration at SPEAR, the electron-positron colliding beam facility at SLAC. I should like to take this opportunity to thank my colleagues for their many contributions: G. S. Abrams, J.-E. Augustin, A. M. Boyarski, M. Breidenbach, D. Briggs, F. Bulos, W. Chinowsky, J. T. Dakin, G. J. Feldman, G. E. Fischer, C. E. Friedberg, D. Fryberger, G. Goldhaber, G. Hanson, D. L. Hartill, R. J. Hollebeek, B. Jean-Marie, J. A. Kadyk, R. R. Larsen, A. M. Litke, D. Lüke, B. A. Lulu, V. Lüth, D. Lyon, C. C. Morehouse, J. M. Paterson, M. L. Perl, F. M. Pierre, T. P. Pun, P. Rapidis, B. Richter, B. Sadoulet, R. F. Schwitters, W. Tanenbaum, G. H. Trilling, F. Vannucci, J. S. Whitaker, F. C. Winkelmann, J. E. Wiss, and J. E. Zipse.

REFERENCES

1. J.-E. Augustin et al., Nuovo Cimento Letters II, 214 (1969); D. Benaksas et al., Phys. Letters 39B, 289 (1972); V. L. Auslander et al., Sov. J. Nucl. Phys. 9, 69 (1969); J. C. Bizot et al., Phys. Letters 32B, 416 (1970); V. E. Balakin et al., Phys. Letters 34B, 328 (1971).
2. B. Bartoli et al., Phys. Rev. D 6, 2374 (1972).
3. C. Bacci et al., Phys. Letters 44B, 533 (1973).
4. F. Ceradini et al., Phys. Letters 47B, 80 (1973).
5. M. Bernardini et al., Phys. Letters 51B, 200 (1974).
6. A. Litke et al., Phys. Rev. Letters 30, 1189 (1973); G. Tarnopolsky et al., Phys. Rev. Letters 32, 432 (1974).
7. A. M. Boyarski et al., Phys. Rev. Letters 34, 764 (1975).
8. J.-E. Augustin et al., Phys. Rev. Letters 33, 1406 (1974).
9. G. S. Abrams et al., Phys. Rev. Letters 33, 1453 (1974).
10. The relations 1-6 are rather more subtle than they appear, and great caution must be exercised in making quantitative use of these dispersion relations. Evidence of this delicacy is the following thought experiment: Suppose there exists a resonance which has only electromagnetic decays through an intermediate photon, i.e., $e^+e^- \to \gamma \to$ resonance $\to \gamma \to$ final state. By construction this results in an apparent contradiction between Eqs. (2) and (3), because R will not change across the resonance, but σ_T will.
11. J. D. Bjorken, Phys. Rev. 148, 1467 (1966). This paper was a voice in the wilderness. Later references are: S. D. Drell, Proc. XVI Conf. on High Energy Physics, NAL, 1972; and Y. Frishman, Phys. Reports C 13, 1 (1974).

12. K. Wilson, Phys. Rev. 179, 1499 (1969).

13. G. Miller et al., Phys. Rev. D 5, 528 (1972). This summary also contains reference to earlier work.

14. H. Harari, Phys. Letters 57B, 265 (1975); and SLAC-PUB-1589 (1975), submitted to Ann. Phys. (N.Y.).

15. A. M. Boyarski et al., Phys. Rev. Letters 35, 195 (1975).

16. H. Muirhead, Proc. Int. Symposium on $p\bar{p}$ Interactions, Lima Koli, Finland, June 1975.

17. S. J. Brodsky, T. Kinoshita, and H. Terazawa, Phys. Rev. D 4, 1532 (1971); and H. Terazawa, Rev. Mod. Phys. 45, 615 (1973).

18. B. Richter, Proc. XVII Int. Conf. on High Energy Physics, London, July 1974 (SLAC-PUB-1478).

19. J. W. Cronin et al., Phys. Rev. Letters 31, 1426 (1973).

20. A. A. Sokolov and I. M. Ternov, Sov. Phys.–Dokl. 8, 1203 (1964); and V. N. Baier, XLVI Int. School of Physics Enrico Fermi, 1969.

21. J. J. Aubert et al., Phys. Rev. Letters 33, 1404 (1974).

22. An important consequence of this fact is that the quantities plotted are not really cross sections but rather convolutions with the energy resolution of the particular experiment. One must not try to compare the "cross sections" of two different laboratories whose resolutions differ.

23. H. Harari, "ψchology," SLAC-PUB-1514 (unpublished).

24. I. Bars et al., SLAC-PUB-1522 (unpublished).

25. O. W. Greenberg, Proc. Orbis Scientiae II, Coral Gables, Florida, 1975, and Maryland preprint 75-064.

26. A. M. Boyarski et al., Phys. Rev. Letters 34, 1357 (1975); and V. Lüth et al., "Quantum Numbers and Decay Widths of the $\psi(3684)$," SLAC-PUB-1617, to be published in Phys. Rev. Letters.

27. J. L. Basdevant pointed out that he and M. Gourdin have entertained a model where Γ_e itself is the relevant factor for comparison, rather than f^{-2}.

28. A. M. Boyarski et al., Phys. Rev. Letters 34, 762 (1975).

29. Cf. Professor Paoluzi's lecture at this meeting.

30. DASP Collaboration, Phys. Letters 56B, 491 (1975), and private communication, B. Wiik.

31. G. Ringland pointed this out to us.

32. DASP Collaboration, Phys. Letters 53B, 491 (1975).

33. Ibid., 57B, 297 (1975).

34. F. J. Gilman, Proc. VI Int. Conf. on High Energy Physics and Nuclear Structure, Sante Fe, New Mexico, June 1975 (also SLAC-PUB-1600).

35. Gilman argues in ref. 34 that as much as 90% can be accounted, but this accounting does not fall into the "clearly reconstructed" class.

36. E. Hilger et al., HEPL Report 758, submitted to Phys. Rev. Letters.

37. DASP Collaboration, submitted to Phys. Letters.

38. Papers are in preparation at SLAC on the cascade seen at DESY and on reconstructing the intermediate state by observing hadronic decays.

39. B. Wiik, private communication.

40. Even the kind of accounting discussed in footnote 35 does not help reach 100%, so there is a real difference between $\psi(3095)$ and $\psi(3684)$.

FIGURE CAPTIONS

1. Total cross section for $e^+e^- \rightarrow$ hadrons as a function of center-of-mass energy. Data are taken from references 1-7.
2. Ratio of the total cross section for $e^+e^- \rightarrow$ hadrons to the QED cross section for pair production as a function of center-of-mass energy from references 2-7.
3. Invariant mass distributions for various particle hypotheses at w = 4.8 GeV.
4. Mean charged multiplicity corrected for acceptance vs. center-of-mass energy.
5. Diagram for production of hadrons by two photons.
6. Artist's view of SLAC-LBL magnetic detector showing major components.
7. (a) Diagram for $e^-p \rightarrow e^-$ + anything by exchange of a space-like photon.
   (b) Diagram for $e^+e^- \rightarrow$ hadron + anything by single time-like photon annihilation.
8. s $d\sigma/dx$ vs. x for center-of-mass energies = 3.0, 3.8, and 4.8 GeV.
9. $d\sigma/(d^3p/E)$ for center-of-mass energies = 3.0, 3.8, and 4.8 GeV. The lines represent the slope of the data on $pp \rightarrow \pi$ + anything at 90° center of mass and 200 GeV lab energy.
10. $d\sigma/(d^3p/E)$ vs. hadron energy for hadrons identified by time of flight.
11. The relative fractions of π, K, and p yields vs. momentum (a) at w = 3.0 GeV and (b) at w = 4.8 GeV.
12. Azimuthal distribution of hadrons for $x > 0.3$ at w = 7.38 and 6.18 GeV. No beam polarization is expected at 6.18 GeV.
13. Cross sections for $e^+e^- \rightarrow$ hadrons, $\mu^+\mu^-$, and e^+e^- vs. center-of-mass energy near the $\psi(3095)$.

14. Cross sections for $e^+e^- \rightarrow$ hadrons, $\mu^+\mu^-$, and e^+e^- vs. center-of-mass energy near $\psi(3684)$.

15. Argand plot of the two amplitudes contributing to μ pair yield near the resonance.

16. Total hadronic cross section (in arbitrary units) vs. center-of-mass energy in fine steps. The only clear peak is the $\psi(3684)$.

17. Ratio of μ pair cross section to e pair cross section as a function of center-of-mass energy near the $\psi(3095)$ and $\psi(3684)$ resonances.

18. Polar angle distribution for e pairs and μ pairs near the peak of the $\psi(3095)$. The solid points represent the measured cross sections, while the open points represent the cross sections after subtracting the QED cross section.

19. Polar angle distribution for e pairs and μ pairs near the peak of the $\psi(3684)$. The solid line is the expected angular distribution for QED plus the resonance, while the dotted line represents QED alone.

20. Front-back polar angle asymmetry for μ pairs vs. center-of-mass energy near the $\psi(3095)$ and $\psi(3684)$ resonances.

21. The relative fractions of π, K, and p yields vs. momentum at the $\psi(3095)$. (Cf. Fig. 11.)

22. Test for direct decays of $\psi(3095)$ to all pions. The ratio, α, plotted should be unity for pure second order electromagnetic decays, greater than unity for direct decays.

23. Missing mass to hypothesis $e^+e^- \rightarrow \pi^+\pi^-\pi^+\pi^-$ X (a) for w = 3.0 GeV and (b) for $\psi(3095)$. The dotted line is an estimate of the background under the peak.

24. Dalitz plot for $\psi(3095) \rightarrow \pi^+\pi^-\pi^0$.

25. Single particle mass for pairs of particles as reconstructed by kinematics.

26. Momentum of reconstructed Λ vs. momentum of reconstructed $\bar{\Lambda}$. Peak at 1.07 GeV/c shows elastic production.

27. Cascade $\psi(3684) \rightarrow \pi^+\pi^-\psi(3095)$, where the $\psi(3095)$ decays into an e^+e^- pair.

28. Total energy distribution for two prong events under the hypothesis of $\rho\pi$ (a) for $\psi(3095)$ and (b) for $\psi(3684)$.

29. Scatter plot of missing momentum vs. observed total energy assuming pion masses. (a) $\psi(3095) \rightarrow$ anything, (b) $\psi(3684) \rightarrow$ anything, (c) $\psi(3684) \rightarrow \psi(3095) + \pi^+\pi^-$, and (d) $\psi(3684) \rightarrow$ anything but with cascade decays removed.

TABLE I

Largest upper limits at the 90% confidence level for inclusive production cross section times branching ratio (nb).

Decay Mode	Mass Region (GeV/c^2)		
	1.50 to 1.85	1.85 to 2.40	2.40 to 4.00
$K^-\pi^+$ and $K^+\pi^-$	0.25	0.18	0.08
$K^0_S\pi^+\pi^-$	0.57	0.40	0.29
$\pi^+\pi^-$	0.13	0.13	0.09
K^+K^-	0.23	0.12	0.10
$K^-\pi^+\pi^+$ and $K^+\pi^-\pi^-$	0.51	0.49	0.19
$K^0_S\pi^+$ and $K^0_S\pi^-$	0.26	0.27	0.09
$K^0_SK^+$ and $K^0_SK^-$	0.54	0.33	0.09
$\pi^+\pi^-\pi^+$ and $\pi^+\pi^-\pi^-$	0.48	0.38	0.18
$K^\mp\pi^\pm$, $\bar{K}^0\pi^+\pi^-$ and $K^0\pi^+\pi^-$	1.16	0.90	0.58
K^+K^- and $\pi^+\pi^-$	0.23	0.16	0.15
$K^\mp\pi^\pm\pi^\pm$, $\bar{K}^0\pi^\pm$ and $K^0\pi^\pm$	0.64	0.51	0.30
$\bar{K}^0K^\pm$, $K^0K^\pm$ and $\pi^+\pi^-\pi^\pm$	1.10	0.76	0.29

TABLE II

Properties of the ψ-particle as obtained from fit to cross sections σ_H, $\sigma_{\mu\mu}$, and σ_{ee}, and reconstruction of multihadron final states.

	$\psi(3095)$	$\psi(3684)$
Mass	3.095 ± 0.004 GeV	3.684 ± 0.005 GeV
$J^{PC}\ I^G$	1^{--} 0^-	1^{--} 0^-
$\Gamma_e = \Gamma_\mu$	4.8 ± 0.6 keV	2.1 ± 0.3 keV
Γ_H	59 ± 14 keV	224 ± 56 keV
Γ	69 ± 15 keV	228 ± 56 keV
Γ_e/Γ	0.069 ± 0.009	0.0093 ± 0.0016
Γ_H/Γ	0.86 ± 0.02	0.981 ± 0.003
Γ_μ/Γ_e	1.00 ± 0.05	0.89 ± 0.16
$\Gamma_{\gamma H}/\Gamma$	0.17 ± 0.03	0.029 ± 0.004

Errors accounted for

(a) statistical

(b) 15% uncertainty on hadron efficiency

(c) 100 keV setting error in $E_{c.m.}$

(d) 2% point-to-point errors, uncorrelated

(e) 3% luminosity normalization

TABLE III

Comparison of Vector Mesons

Particle	Mass GeV	Γ MeV	Γ_e keV	$\left(\frac{f^2}{4\pi}\right)^{-1}$
ρ	0.770 ± 0.010	150 ± 10	6.5 ± 0.5	0.48 ± 0.04
ω	0.7827 ± 0.0006	10 ± 0.4	0.76 ± 0.17	0.055 ± 0.012
ϕ	1.0197 ± 0.0003	4.2 ± 0.2	1.34 ± 0.08	0.074 ± 0.004
ψ(3095)	3.095 ± 0.004	0.069 ± 0.015	4.8 ± 0.6	0.09 ± 0.01
ψ(3684)	3.684 ± 0.005	0.228 ± 0.056	2.1 ± 0.3	0.032 ± 0.005
?(4100)	4.15 ± 0.1	250 → 300	4 ± 1	0.05 ± 0.02

TABLE IV

Results of the search for narrow resonances. Upper limits (90% confidence level) for the radiatively corrected integrated cross section of a possible narrow resonance. The width of this resonance is assumed to be small compared to the mass resolution.

Mass Range (GeV)	Limit on $\int\sigma_H\, dw$ (nb MeV)
3.20 → 3.50	970
3.50 → 3.69	780
3.72 → 4.00	850
4.00 → 4.40	620
4.40 → 4.90	580
4.90 → 5.40	780
5.40 → 5.90	800
5.90 → 7.60	450

TABLE V

Decay Modes of $\psi(3095)$

Mode	Branching Ratio (%)	Reference or Note
e^+e^-	6.9 ± 0.9	
$\mu^+\mu^-$	6.9 ± 0.9	
$\gamma\gamma$	< 0.34	32
$\gamma\pi^o$	< 0.9	32
$\gamma\eta$	$0.7^{+2}_{-0.6}$	39
$\pi^+\pi^-$	< 0.032	33*
$2\pi^+2\pi^-$	0.4 ± 0.1	Compatible with vacuum polarization
$3\pi^+3\pi^-$	0.4 ± 0.2	Compatible with vacuum polarization
$\rho\pi$	1.3 ± 0.3	$\geq$ 70% of $\pi^+\pi^-\pi^o$
$2\pi^+2\pi^-\pi^o$	4.0 ± 1.0	$\begin{cases} 20\% \ \omega\pi^+\pi^- \\ 30\% \ \rho\pi\pi\pi \end{cases}$
$3\pi^+3\pi^-\pi^o$	2.9 ± 0.7	
$4\pi^+4\pi^-\pi^o$	0.9 ± 0.3	
K^+K^-	< 0.06	33*
K_SK_L	< 0.02	
$K^{*o}(892)\overline{K^{*o}}(892)$	< 0.06	
$K^{*o}(1420)\overline{K^{*o}}(1420)$	< 0.18	
$K^o\overline{K^{*o}}(892) + \overline{K^o}K^{*o}(892)$	0.24 ± 0.05	
$K^+K^{*-}(892) + K^-K^{*+}(892)$	0.31 ± 0.07	
$K^o\overline{K^{*o}}(1420) + \overline{K^o}K^{*o}(1420)$	< 0.19	
$K^+K^{*-}(1420) + K^-K^{*+}(1420)$	< 0.19	
$K^{*o}(892)\overline{K^{*o}}(1420) + \overline{K^{*o}}(892)K^*(1420)$	0.37 ± 0.10	
$K^+K^-\pi^+\pi^-$	0.4 ± 0.2	Excluding K*(892) and K*(1420)
$K^+K^-2\pi^+2\pi^-$	0.3 ± 0.1	
$p\bar{p}$	0.21 ± 0.04	Incompatible with vacuum polarization
$\Lambda\bar{\Lambda}$	0.16 ± 0.08	
$p\bar{p}\pi^o + p\bar{n}\pi^- + \bar{p}n\pi^+$	0.37 ± 0.19	

Upper limits are 90% confidence

* Using $B(e^+e^-) = 0.069$

TABLE VI

Decay Modes of the $\psi(3684)$

Mode	Branching Ratio (%)	Reference or Note
$e^+e^- = \mu^+\mu^-$	0.97 ± 0.16	
$\gamma\gamma$	$< 1.$	33
$\gamma\pi^o$	$< 1.$	33
$\gamma\eta$	< 0.4	33
$\psi(3095)$ + anything	57 ± 8	
$\psi(3095) + \pi^+\pi^-$	32 ± 4	
$\psi(3095) + \pi^o\pi^o$	20 ± 5	36*
$\psi(3095) + \eta$	4 ± 2	
$\rho^o\pi^o$	< 0.1	
$2\pi^+ 2\pi^-\pi^o$	< 0.7	
$p\bar{p}$	< 0.03	

Upper limits are 90% confidence

* Using $B(\psi(3684) \rightarrow \psi(3095) + \pi^+\pi^-) = 0.32$

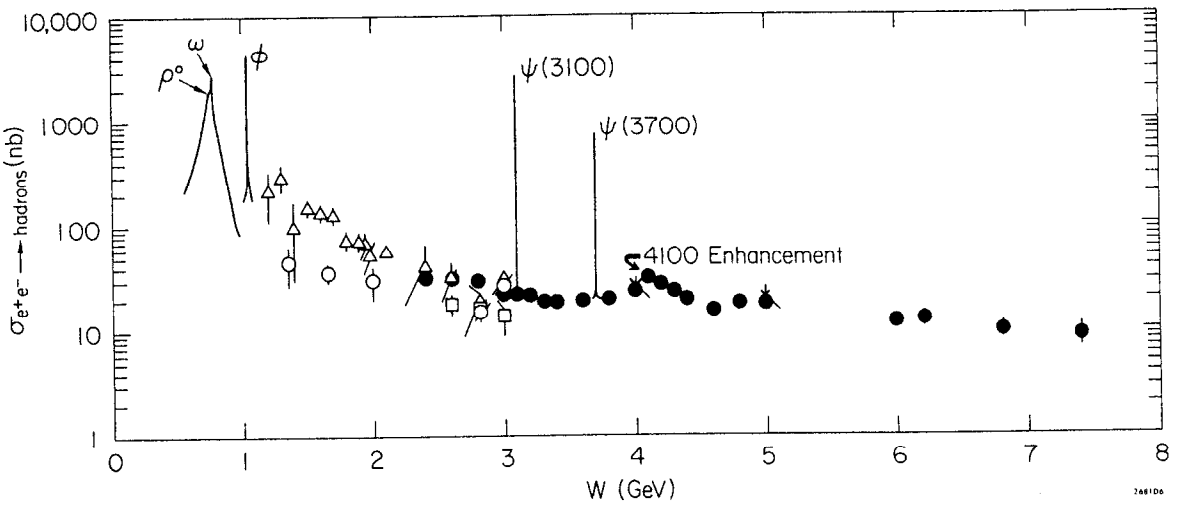
10,000
1000
100
10
1
$\sigma_{e^+e^-\to hadrons}$ (nb)
ρ^0
ω
ϕ
ψ(3100)
ψ(3700)
4100 Enhancement
0
1
2
3
4
5
6
7
8
W (GeV)
2661D6

Fig. 1

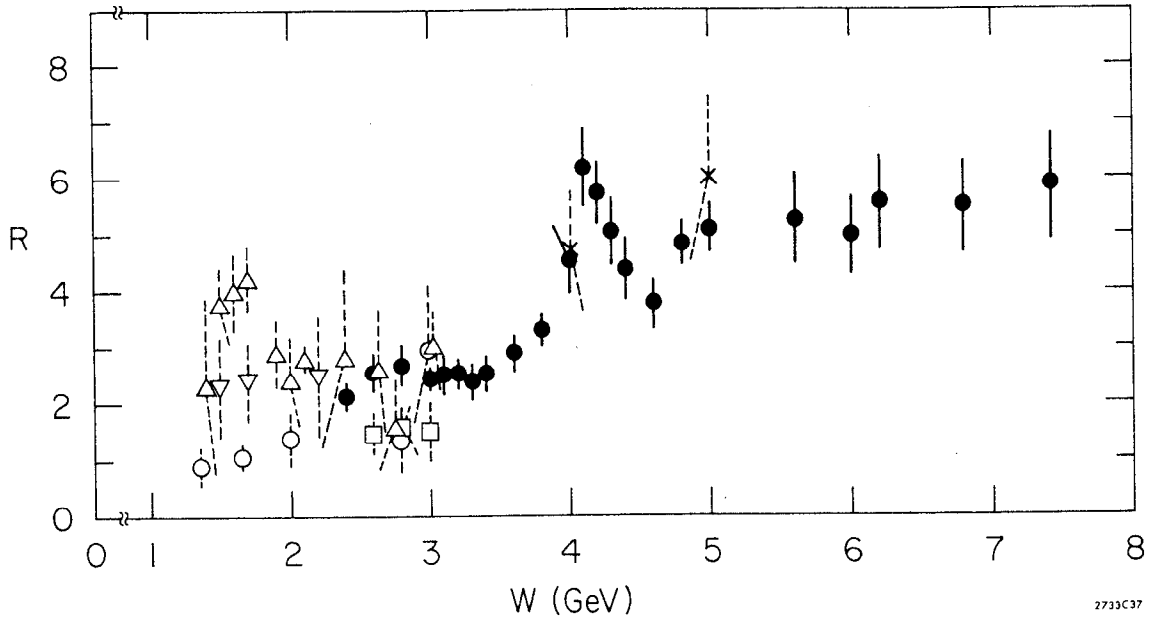
8
6
4
2
0
R
0
1
2
3
4
5
6
7
8
W (GeV)
2733C37

Fig. 2

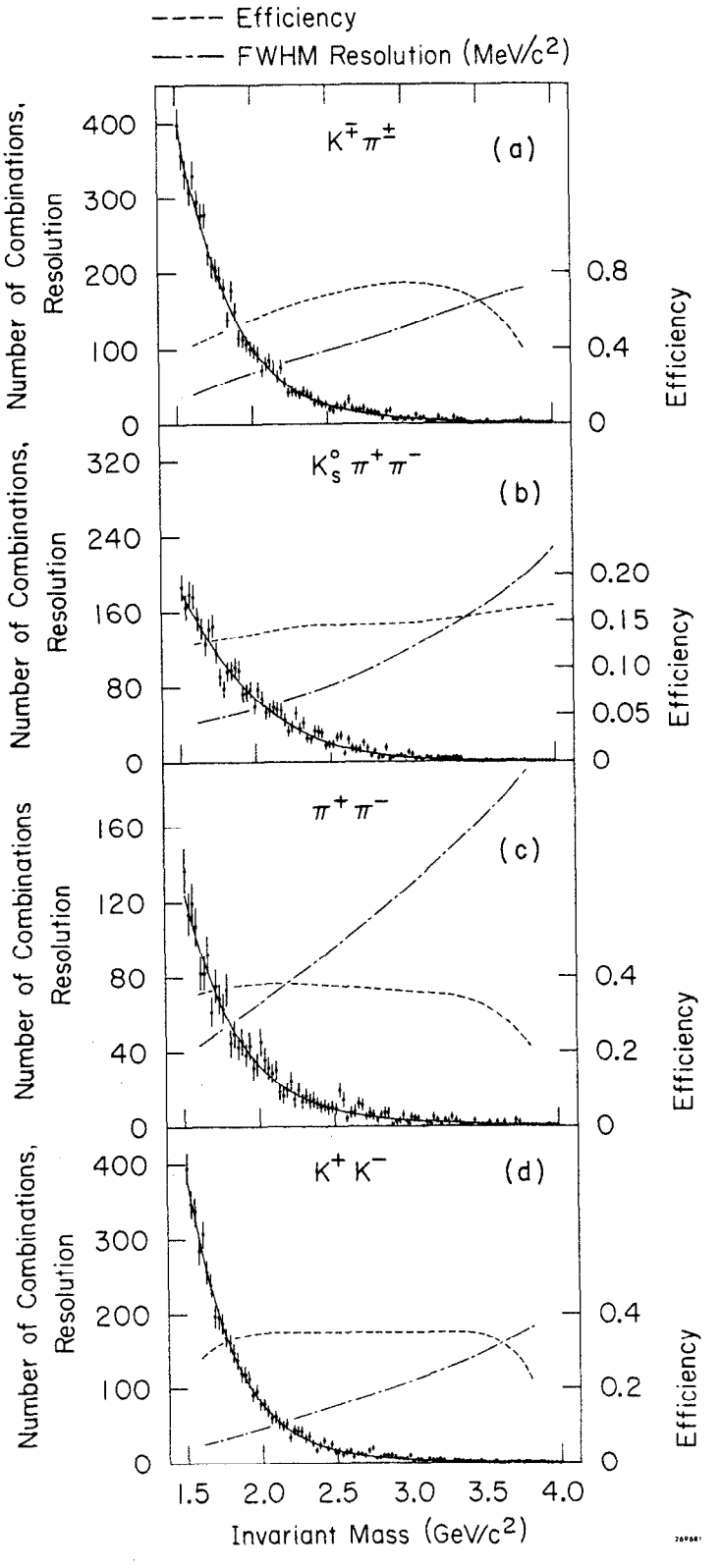
Efficiency
FWHM Resolution (MeV/c²)
Number of Combinations, Resolution
Efficiency
K∓π±
(a)
Ks° π+π−
(b)
π+π−
(c)
K+K−
(d)
Invariant Mass (GeV/c²)

Fig. 3

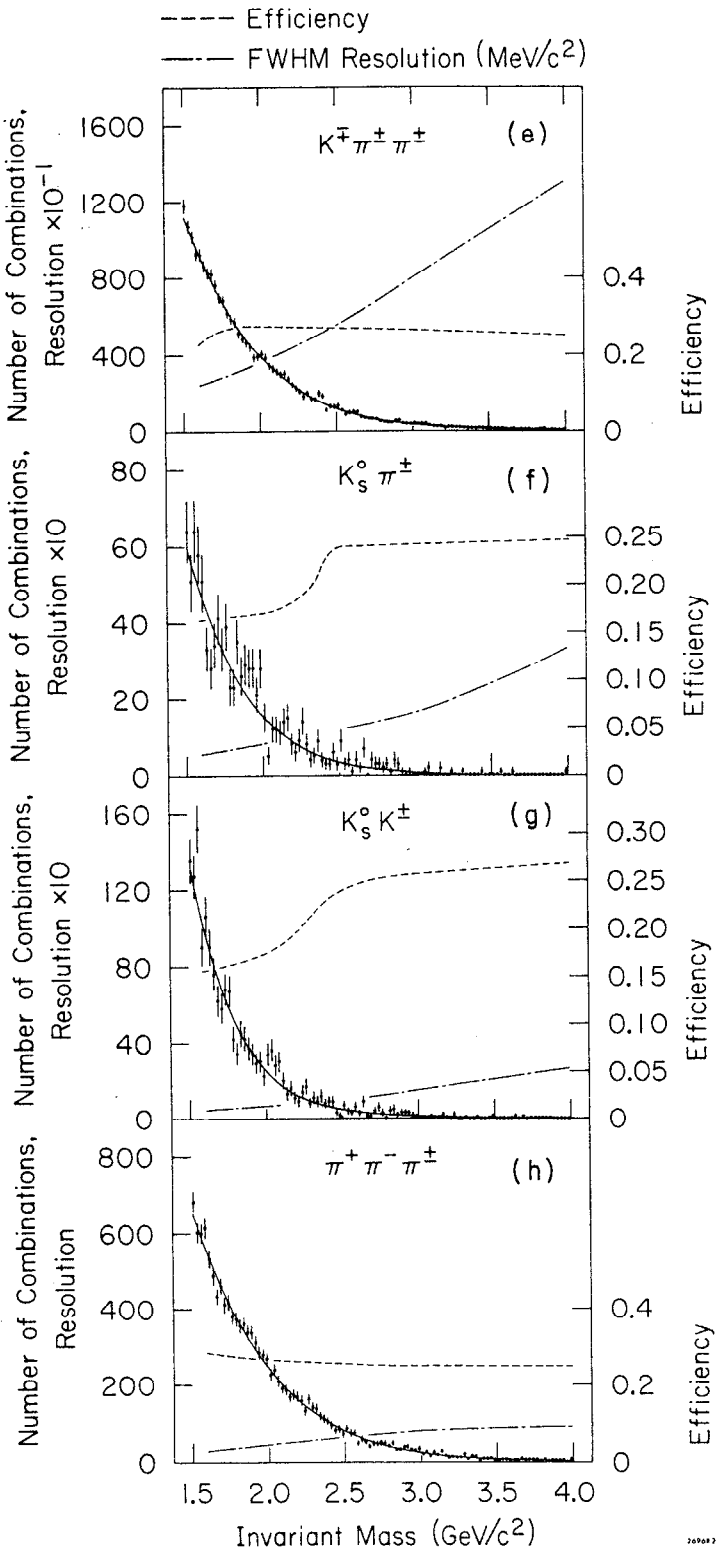
Efficiency
FWHM Resolution (MeV/c²)
$K^{\mp}\pi^{\pm}\pi^{\pm}$ (e)
$K^{\circ}_{s}\pi^{\pm}$ (f)
$K^{\circ}_{s}K^{\pm}$ (g)
$\pi^{+}\pi^{-}\pi^{\pm}$ (h)
Number of Combinations, Resolution ×10⁻¹
Number of Combinations, Resolution ×10
Number of Combinations, Resolution
Efficiency
Invariant Mass (GeV/c²)

Fig. 3 Cont.

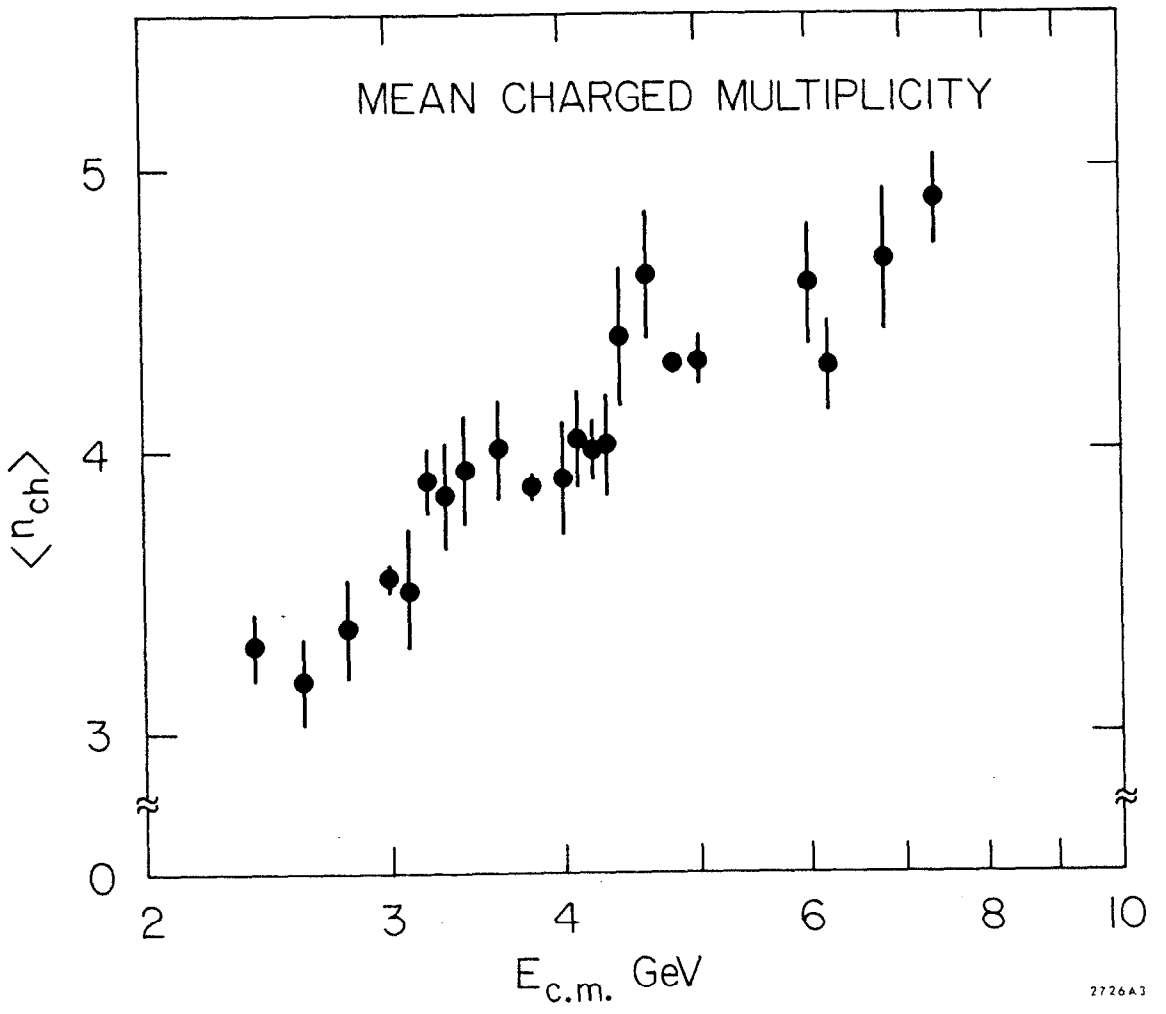
MEAN CHARGED MULTIPLICITY
$\langle n_{ch} \rangle$
0
3
4
5
2
3
4
6
8
10
$E_{c.m.}$ GeV
2726A3

Fig. 4

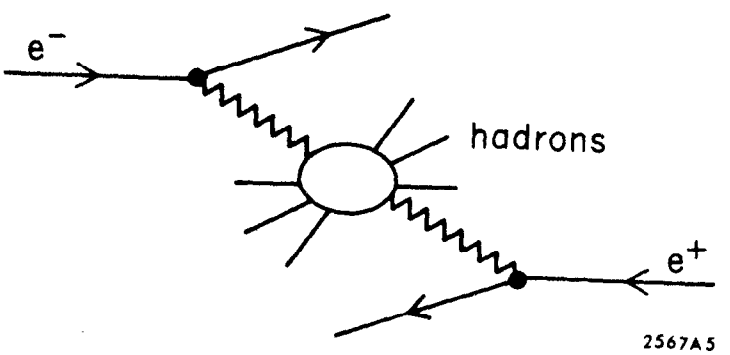

Fig. 5

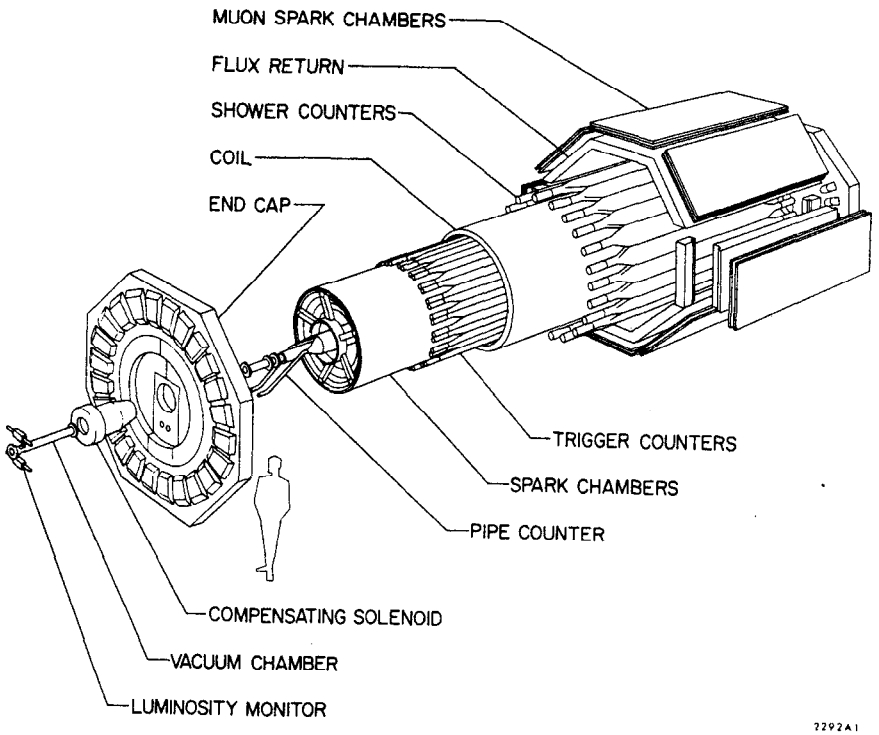
MUON SPARK CHAMBERS
FLUX RETURN
SHOWER COUNTERS
COIL
END CAP
TRIGGER COUNTERS
SPARK CHAMBERS
PIPE COUNTER
COMPENSATING SOLENOID
VACUUM CHAMBER
LUMINOSITY MONITOR
2292A1

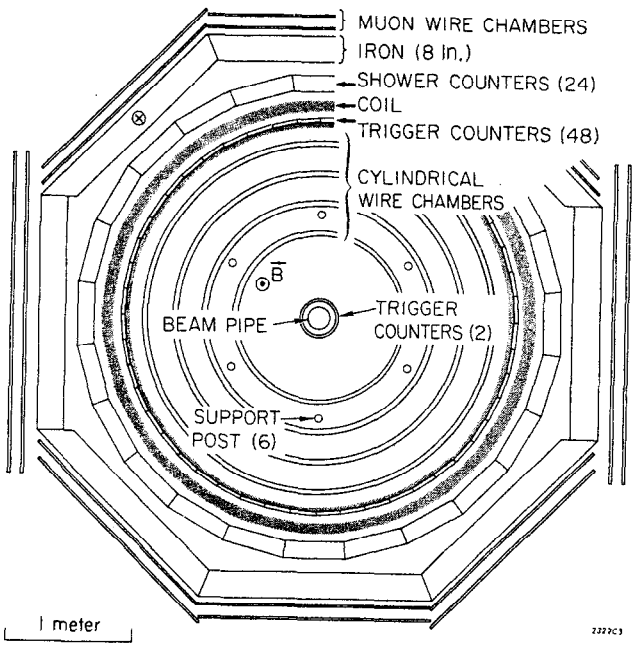
MUON WIRE CHAMBERS
IRON (8 In.)
SHOWER COUNTERS (24)
COIL
TRIGGER COUNTERS (48)
CYLINDRICAL
WIRE CHAMBERS
B
BEAM PIPE
TRIGGER
COUNTERS (2)
SUPPORT
POST (6)
1 meter

Fig. 6

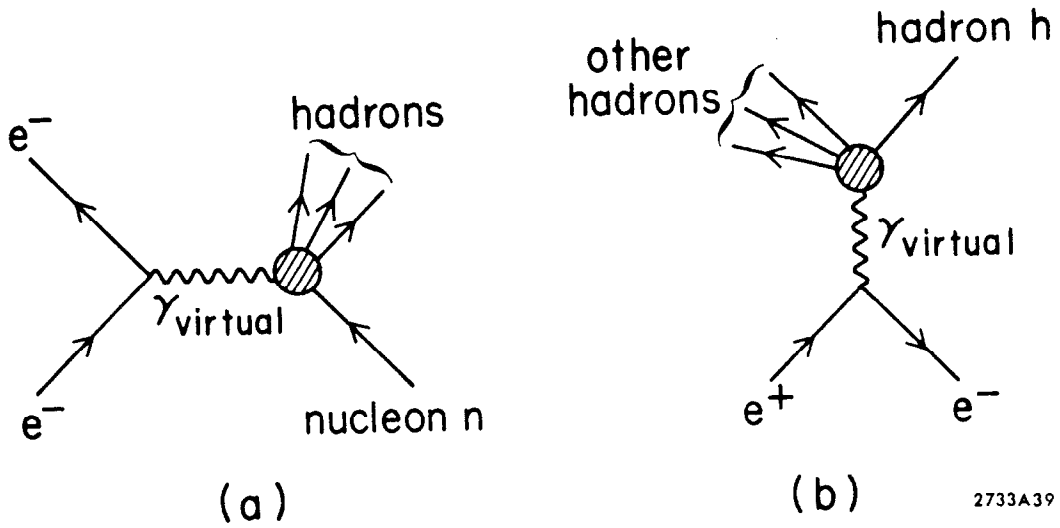
e⁻
hadrons
γ virtual
e⁻
nucleon n
(a)
other hadrons
hadron h
γ virtual
e⁺
e⁻
(b)
2733A39

Fig. 7

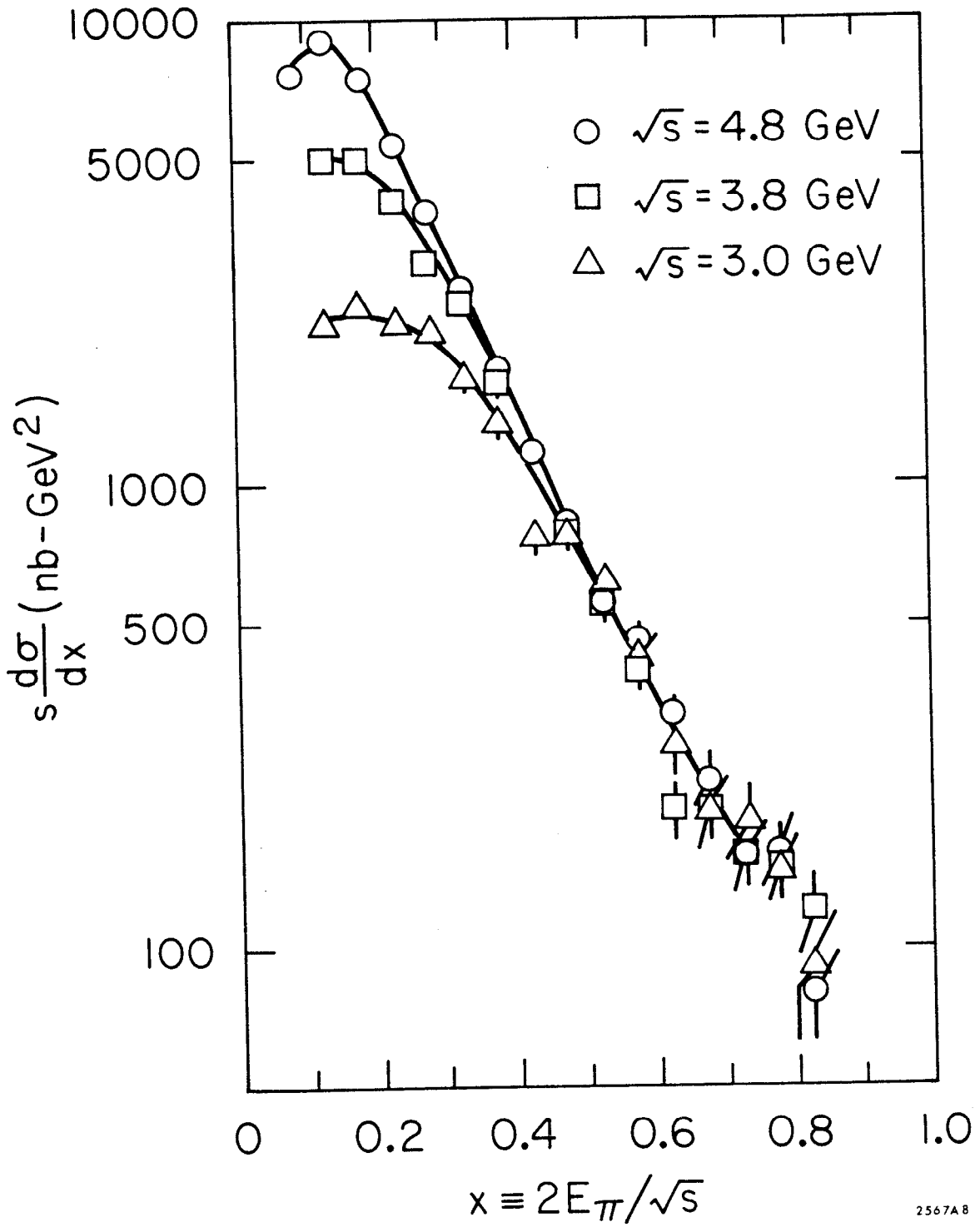
10000
5000
1000
500
100
$s\frac{d\sigma}{dx}$ (nb-GeV^2)
$\sqrt{s}$ = 4.8 GeV
$\sqrt{s}$ = 3.8 GeV
$\sqrt{s}$ = 3.0 GeV
0
0.2
0.4
0.6
0.8
1.0
$x \equiv 2E_\pi/\sqrt{s}$
2567A8

Fig. 8

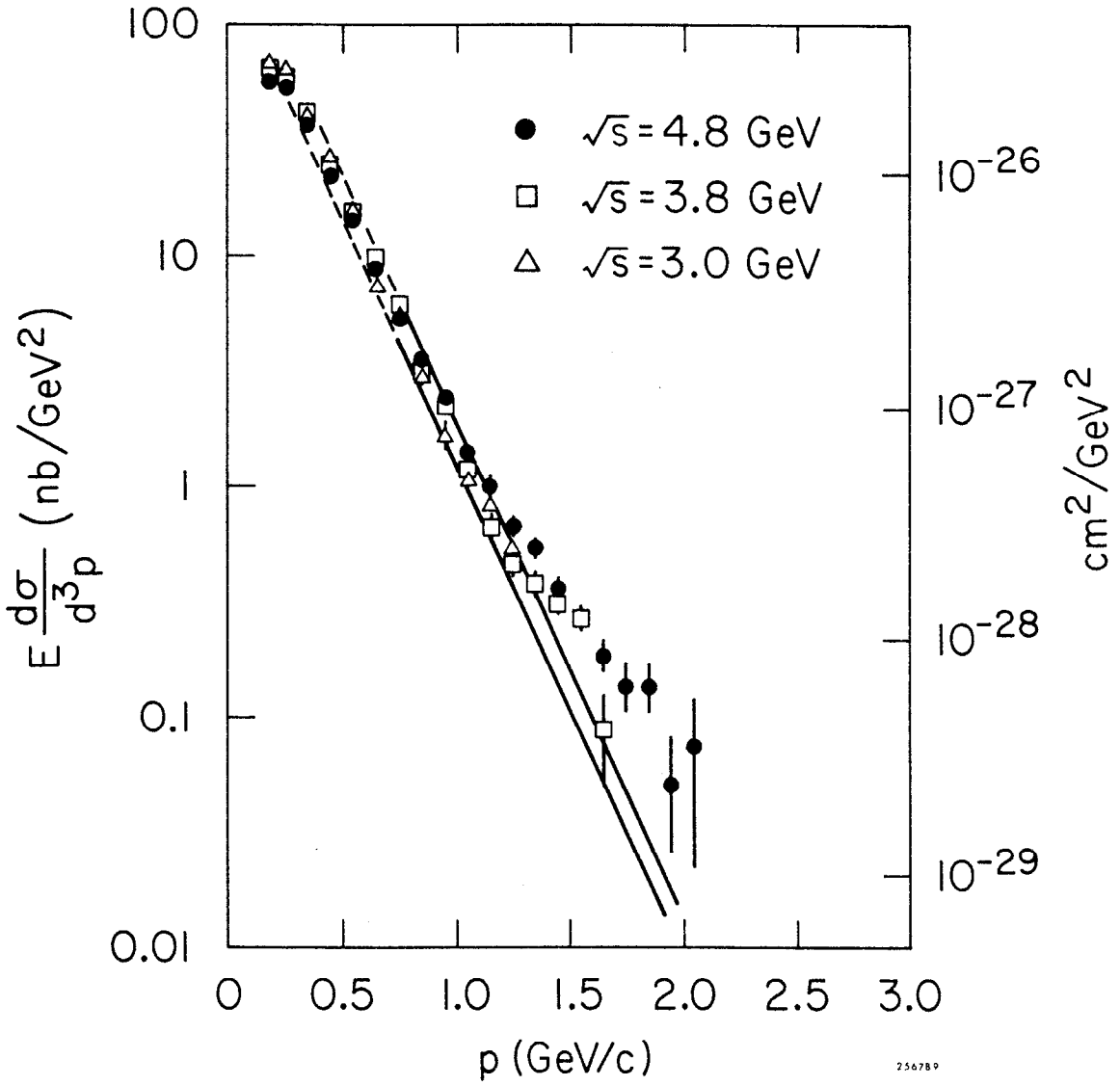
100
10
1
0.1
0.01
$E\frac{d\sigma}{d^3p}$ (nb/GeV^2)
$\sqrt{s}$ = 4.8 GeV
$\sqrt{s}$ = 3.8 GeV
$\sqrt{s}$ = 3.0 GeV
10^{-26}
10^{-27}
10^{-28}
10^{-29}
cm^2/GeV^2
0
0.5
1.0
1.5
2.0
2.5
3.0
p (GeV/c)
256789

Fig. 9

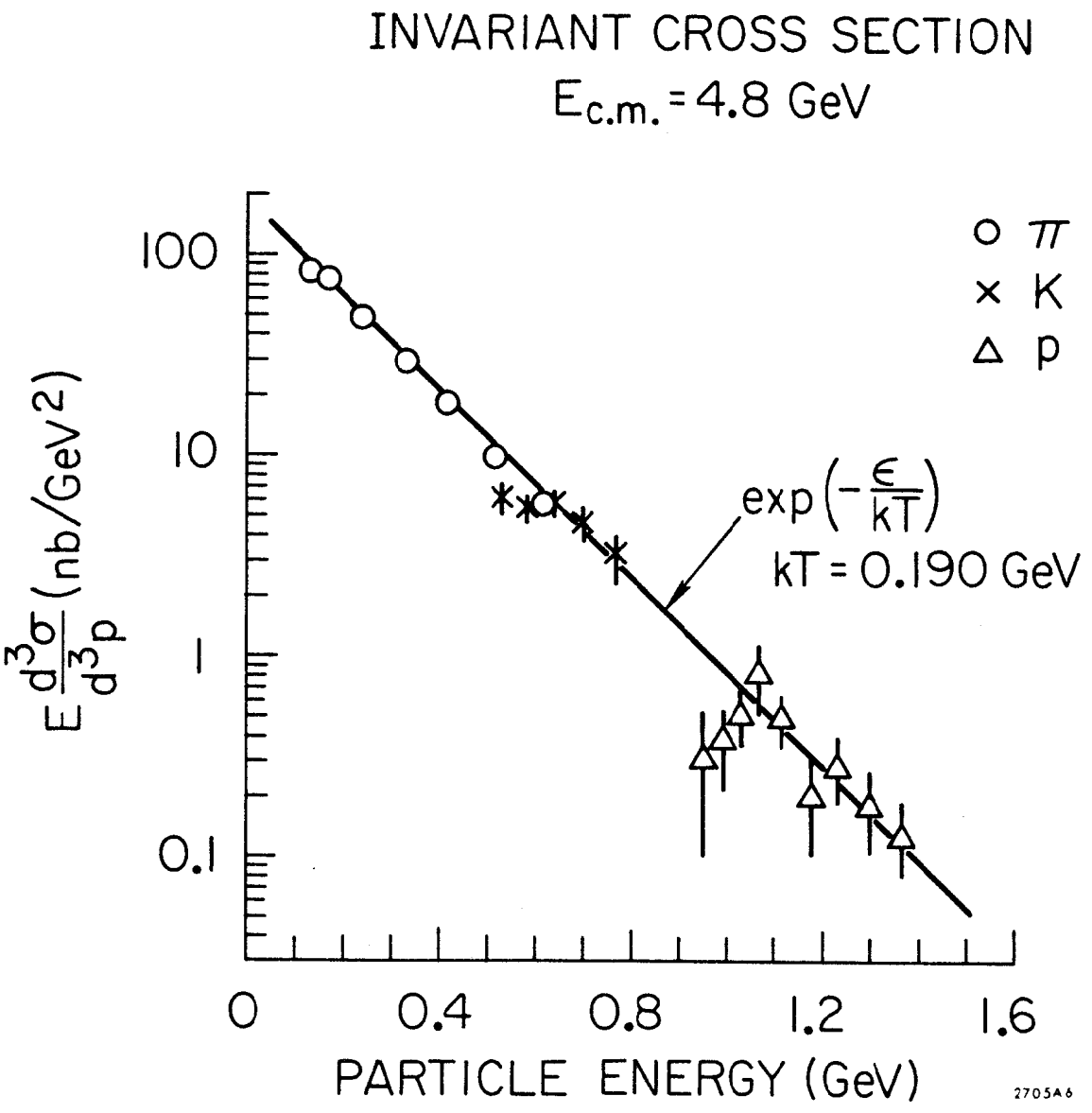
INVARIANT CROSS SECTION
$E_{c.m.} = 4.8$ GeV
$E\frac{d^3\sigma}{d^3p}$ (nb/GeV^2)
100
10
1
0.1
0
0.4
0.8
1.2
1.6
PARTICLE ENERGY (GeV)
o π
× K
Δ p
$\exp\left(-\frac{\epsilon}{kT}\right)$
kT = 0.190 GeV
2705A6

Fig. 10

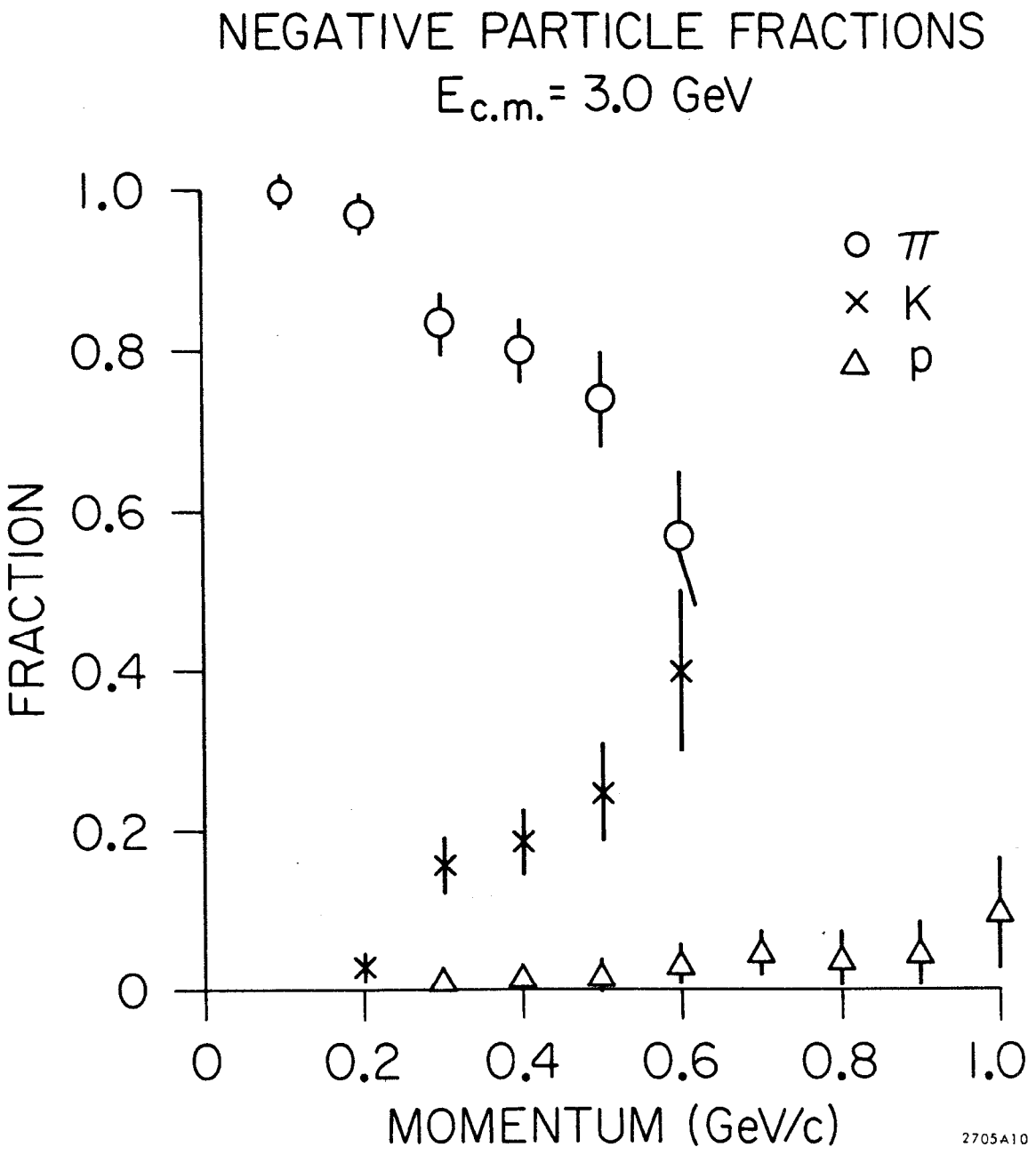
NEGATIVE PARTICLE FRACTIONS
$E_{c.m.}$ = 3.0 GeV
1.0
0.8
0.6
0.4
0.2
0
FRACTION
o π
× K
△ p
0
0.2
0.4
0.6
0.8
1.0
MOMENTUM (GeV/c)
2705A10

Fig. 11a

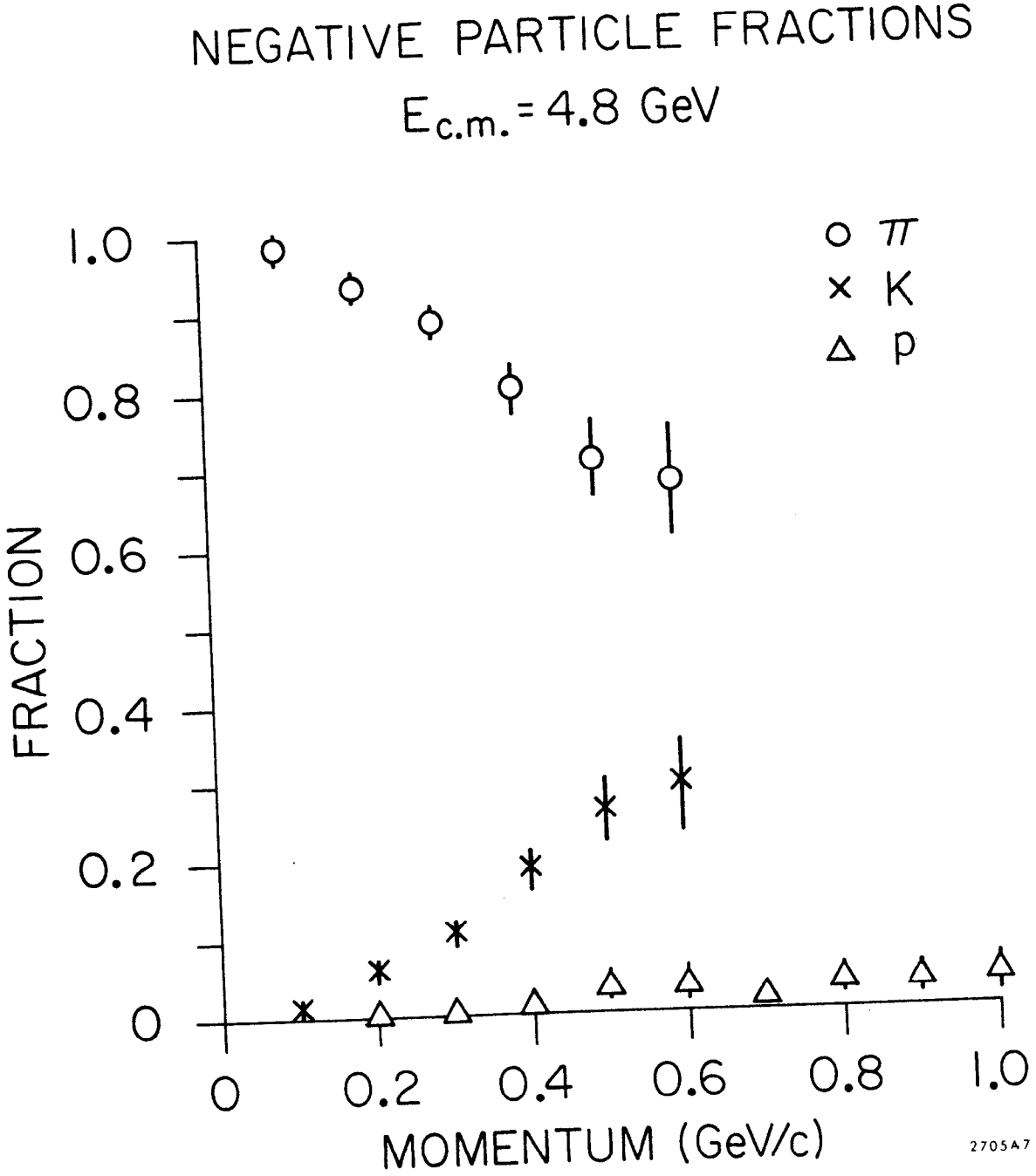
NEGATIVE PARTICLE FRACTIONS
$E_{c.m.} = 4.8$ GeV
π
K
p
FRACTION
1.0
0.8
0.6
0.4
0.2
0
0
0.2
0.4
0.6
0.8
1.0
MOMENTUM (GeV/c)
2705A7

Fig. 11b

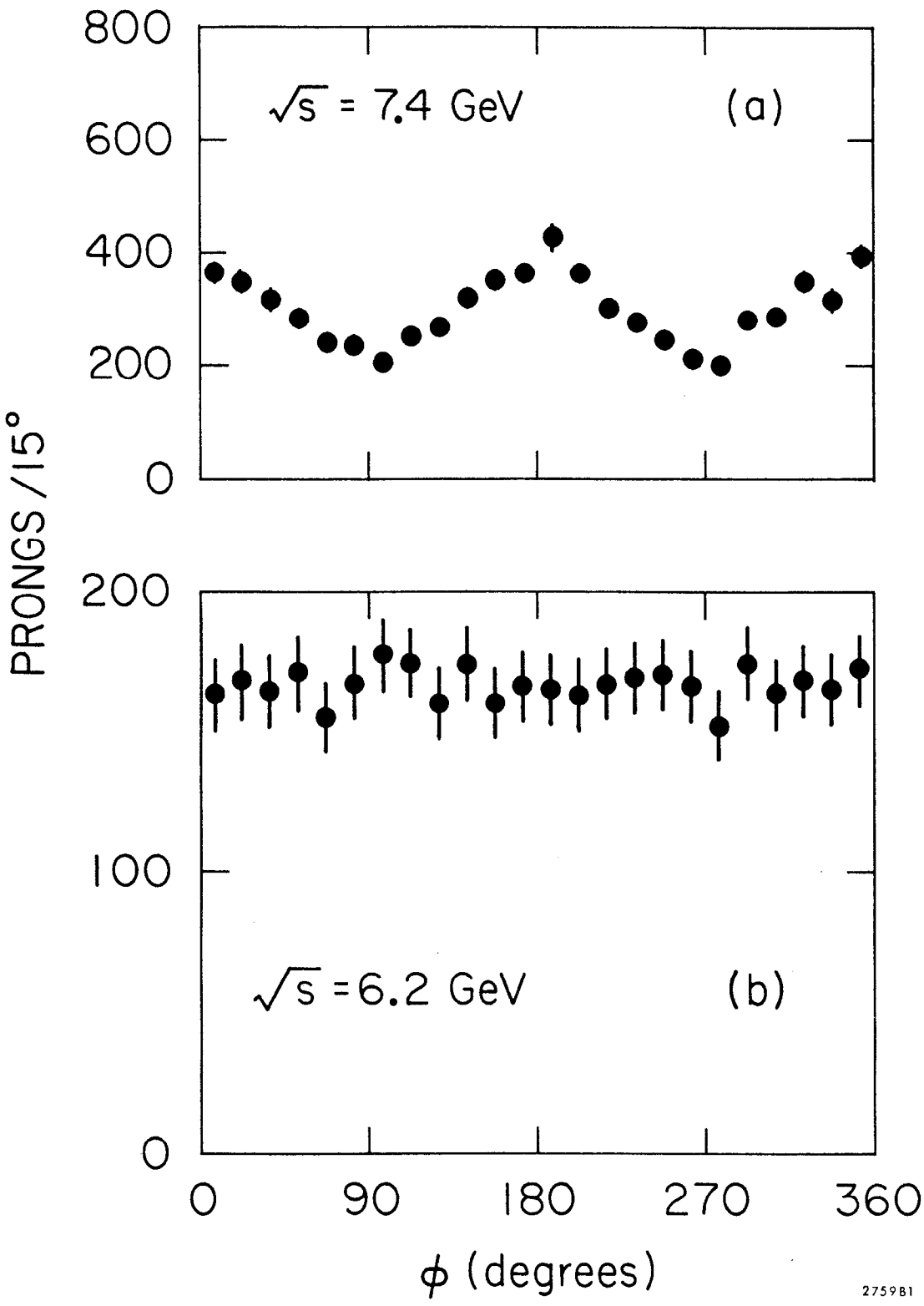
800
600
400
200
0
√s = 7.4 GeV
(a)
200
100
0
√s = 6.2 GeV
(b)
PRONGS / 15°
0
90
180
270
360
φ (degrees)
2759B1

Fig. 12

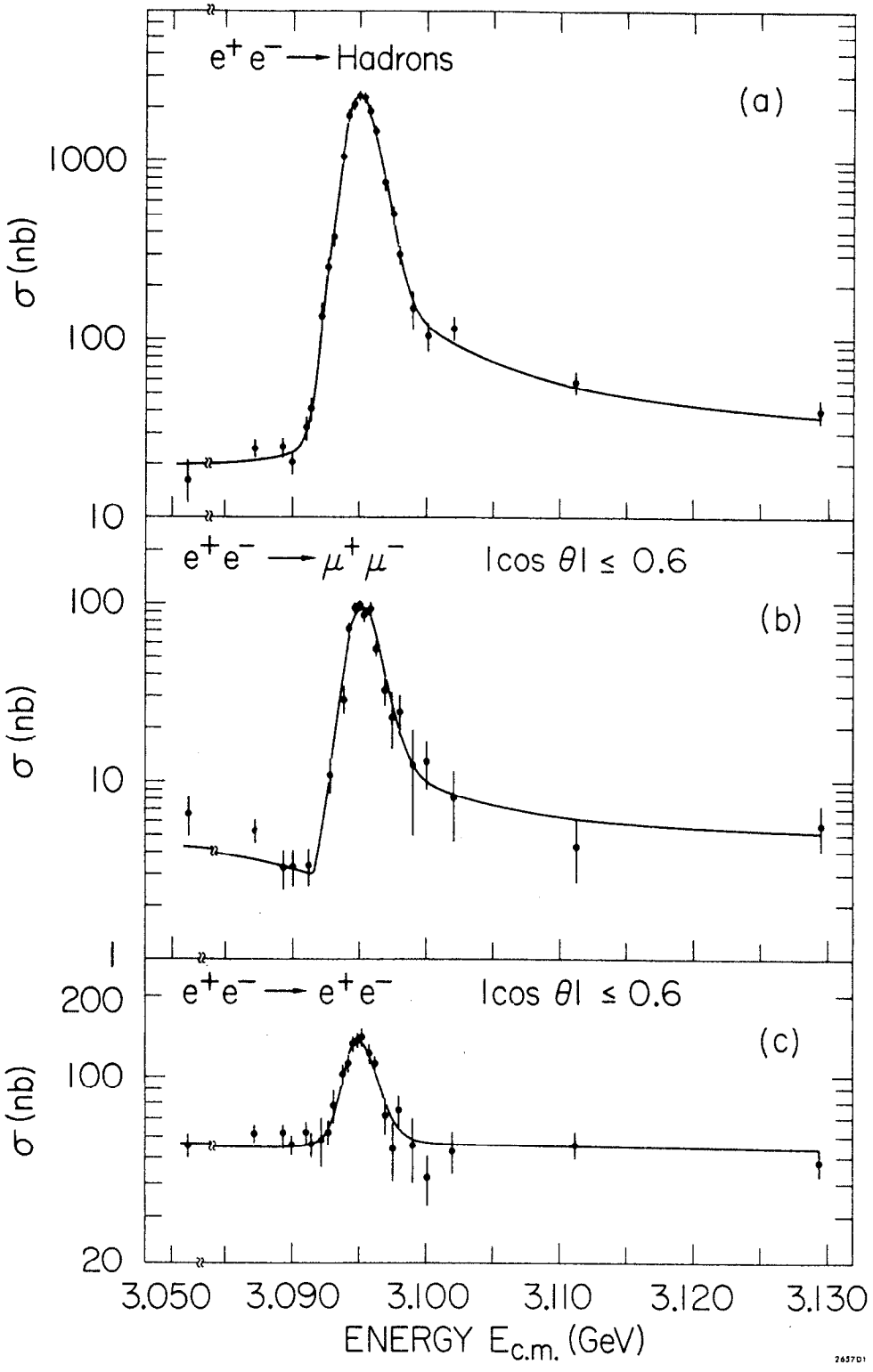
e+ e− → Hadrons
(a)
1000
100
10
σ (nb)
e+e− → μ+μ−
|cos θ| ≤ 0.6
(b)
100
10
1
σ (nb)
e+e− → e+e−
|cos θ| ≤ 0.6
(c)
200
100
20
σ (nb)
3.050
3.090
3.100
3.110
3.120
3.130
ENERGY Ec.m. (GeV)
265701

Fig. 13

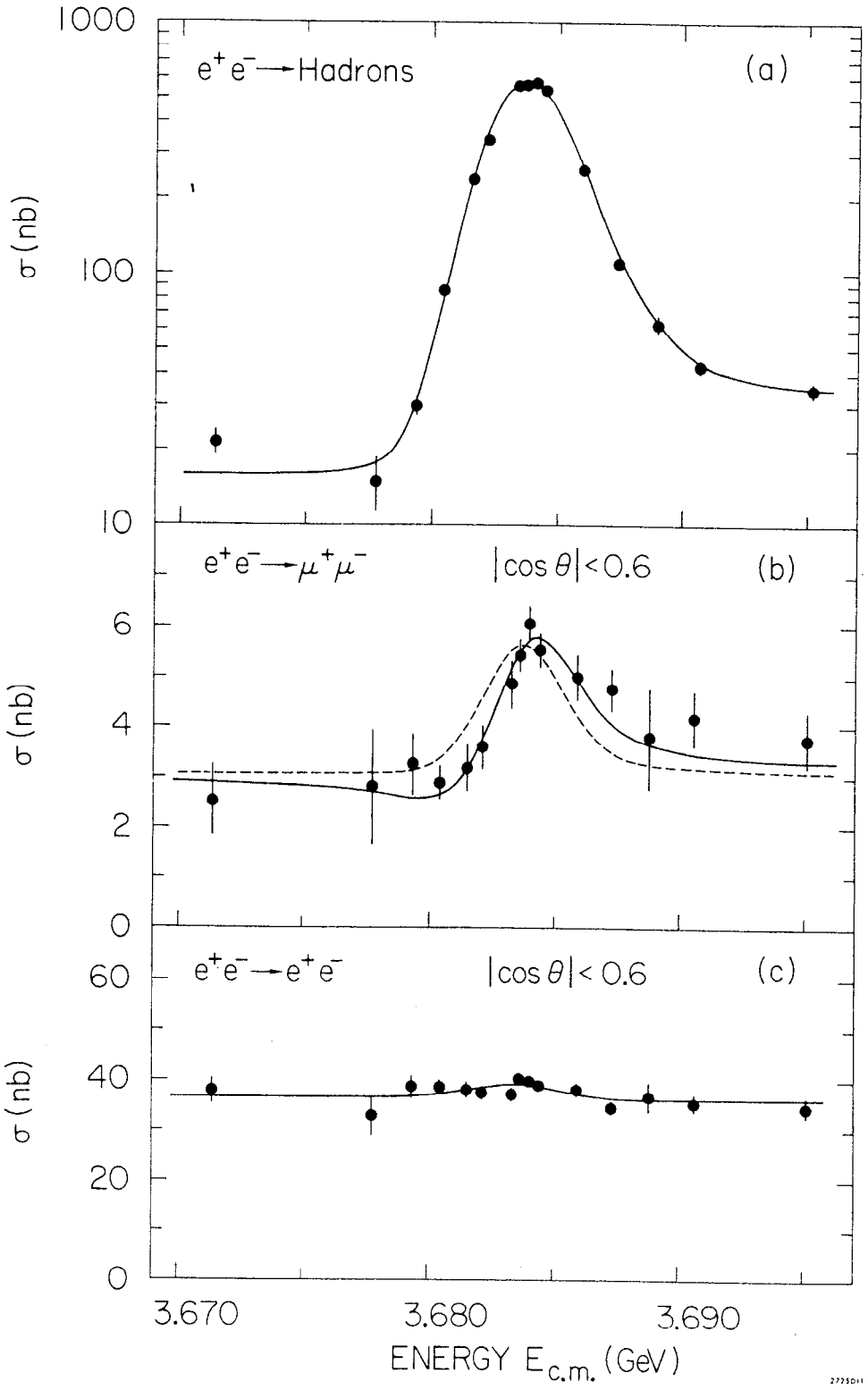
1000
100
10
σ (nb)
e+e−→Hadrons
(a)
e+e−→μ+μ−
|cos θ|<0.6
(b)
6
4
2
0
σ (nb)
e+e−→e+e−
|cos θ|<0.6
(c)
60
40
20
0
σ (nb)
3.670
3.680
3.690
ENERGY Ec.m. (GeV)

Fig. 14

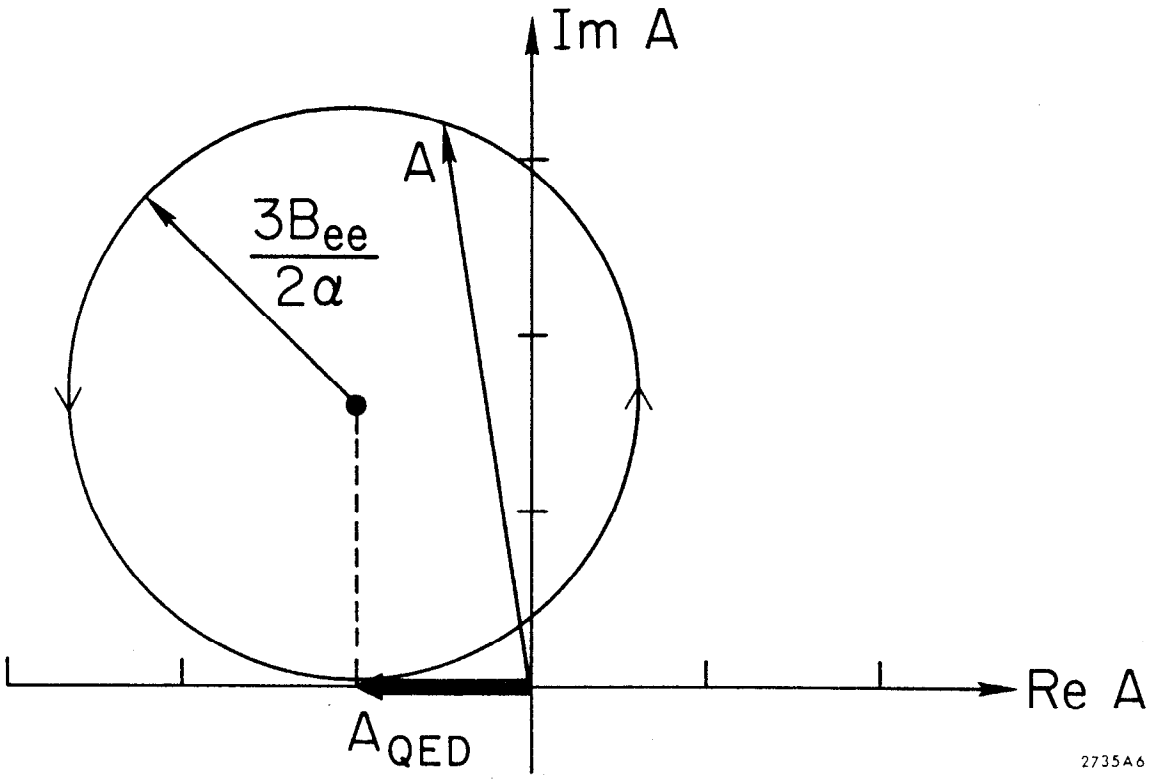

Fig. 15

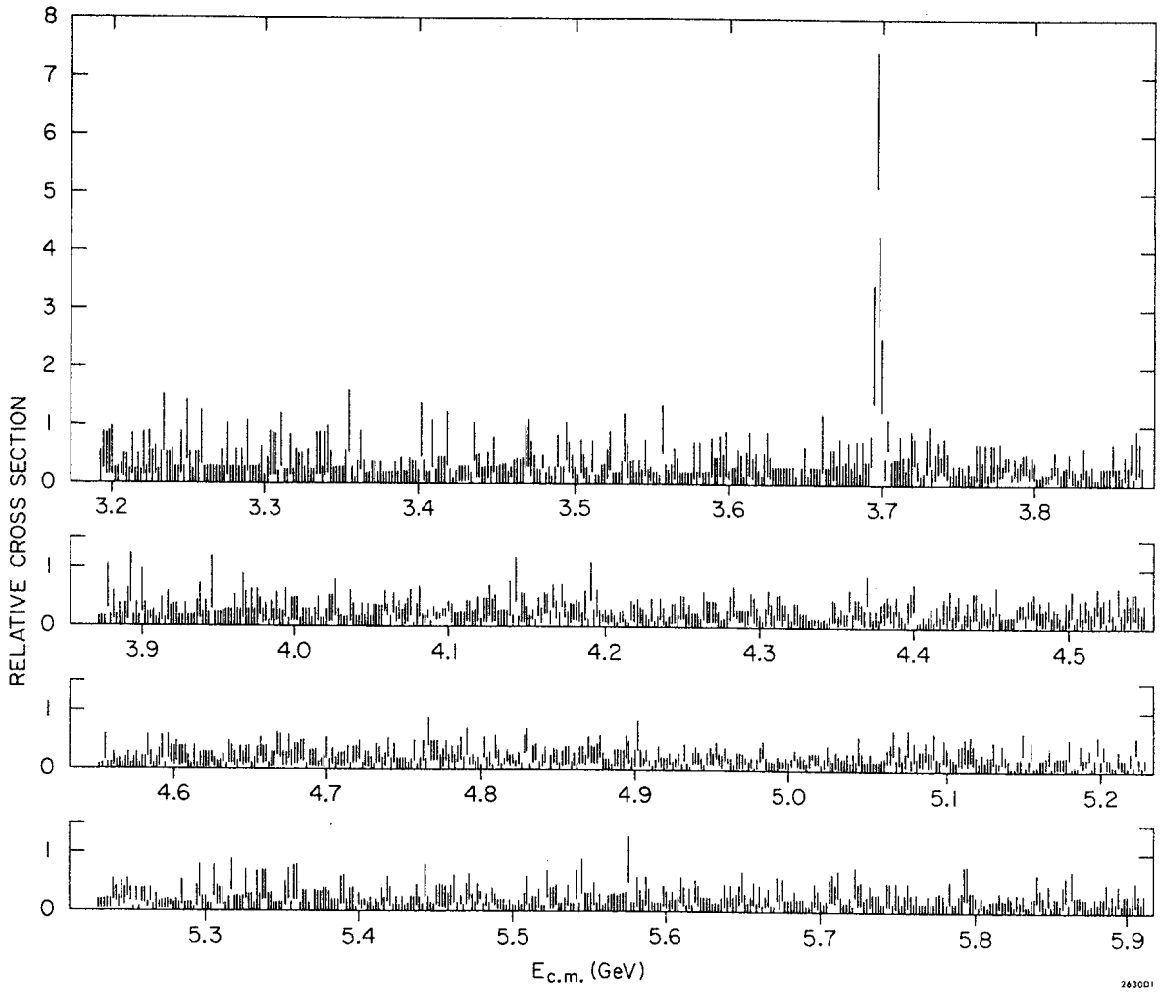
RELATIVE CROSS SECTION
8
7
6
5
4
3
2
1
0
3.2
3.3
3.4
3.5
3.6
3.7
3.8
3.9
4.0
4.1
4.2
4.3
4.4
4.5
4.6
4.7
4.8
4.9
5.0
5.1
5.2
5.3
5.4
5.5
5.6
5.7
5.8
5.9
$E_{c.m.}$ (GeV)
2630D1

Fig. 16

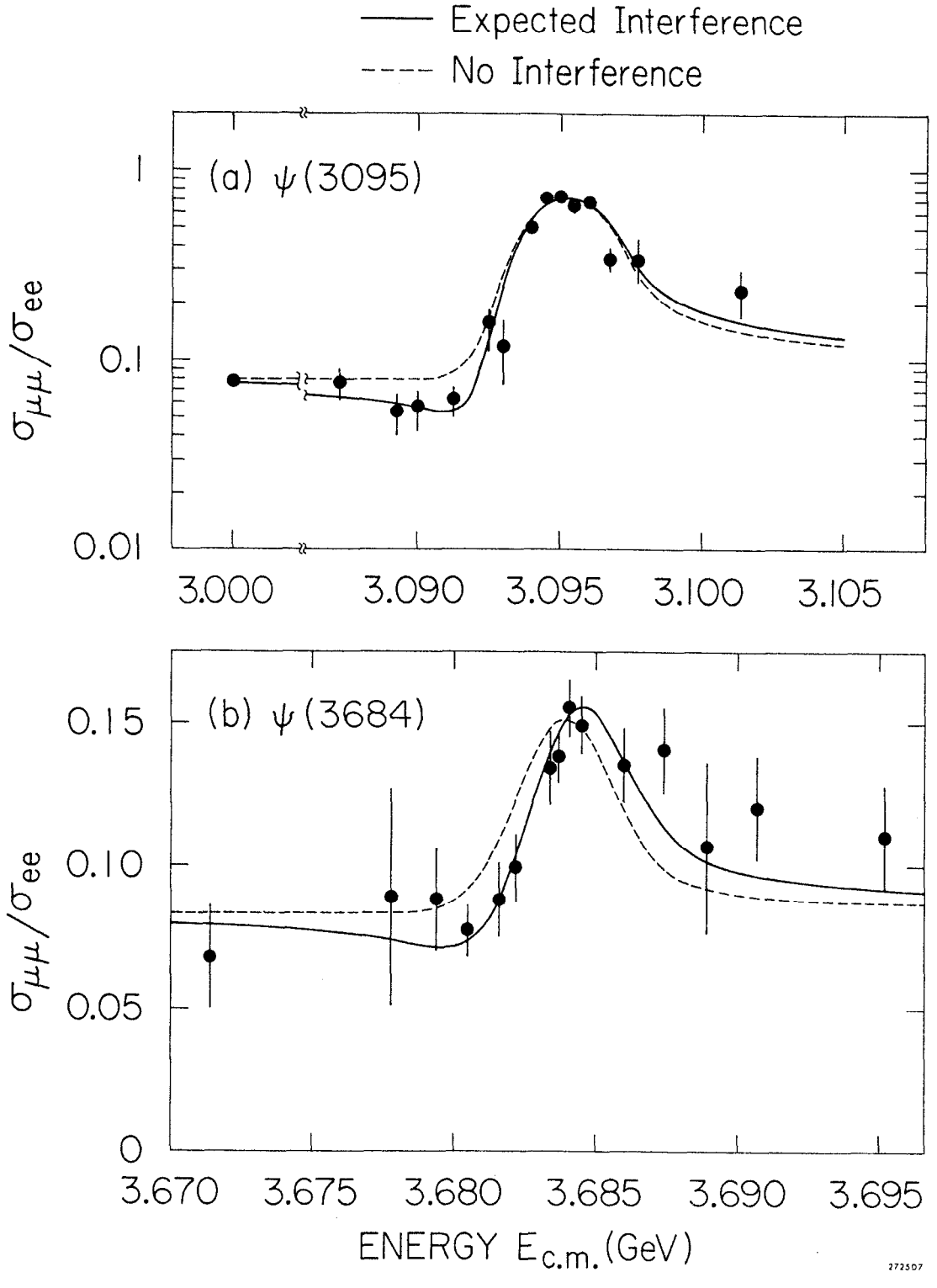
Expected Interference
No Interference
(a) ψ(3095)
1
0.1
0.01
$\sigma_{\mu\mu}/\sigma_{ee}$
3.000
3.090
3.095
3.100
3.105
(b) ψ(3684)
0.15
0.10
0.05
0
$\sigma_{\mu\mu}/\sigma_{ee}$
3.670
3.675
3.680
3.685
3.690
3.695
ENERGY $E_{c.m.}$ (GeV)
272507

Fig. 17

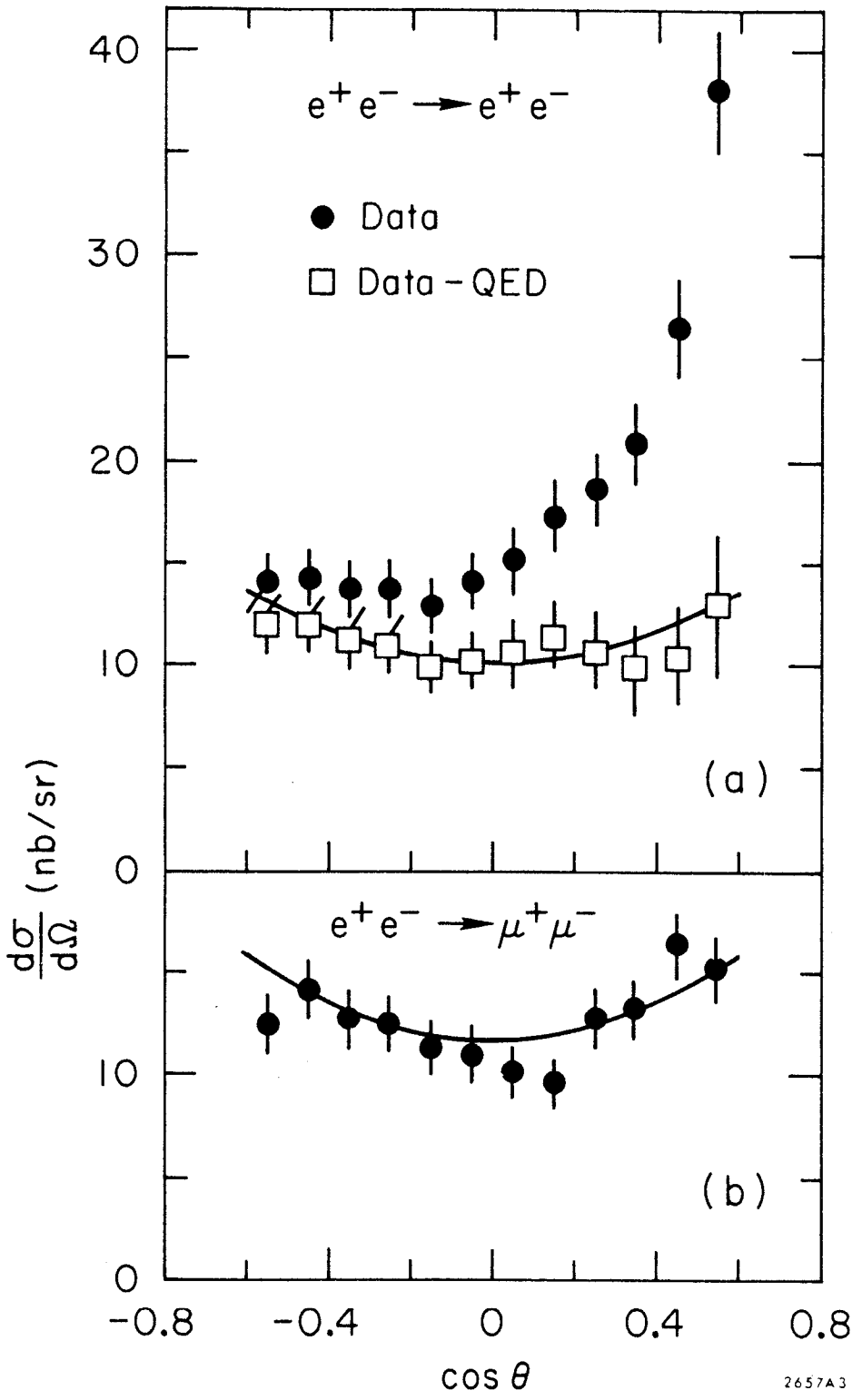
40
30
20
10
0
$e^+e^- \rightarrow e^+e^-$
Data
Data - QED
(a)
$\frac{d\sigma}{d\Omega}$ (nb/sr)
$e^+e^- \rightarrow \mu^+\mu^-$
10
0
(b)
-0.8
-0.4
0
0.4
0.8
cos θ
2657A3

Fig. 18

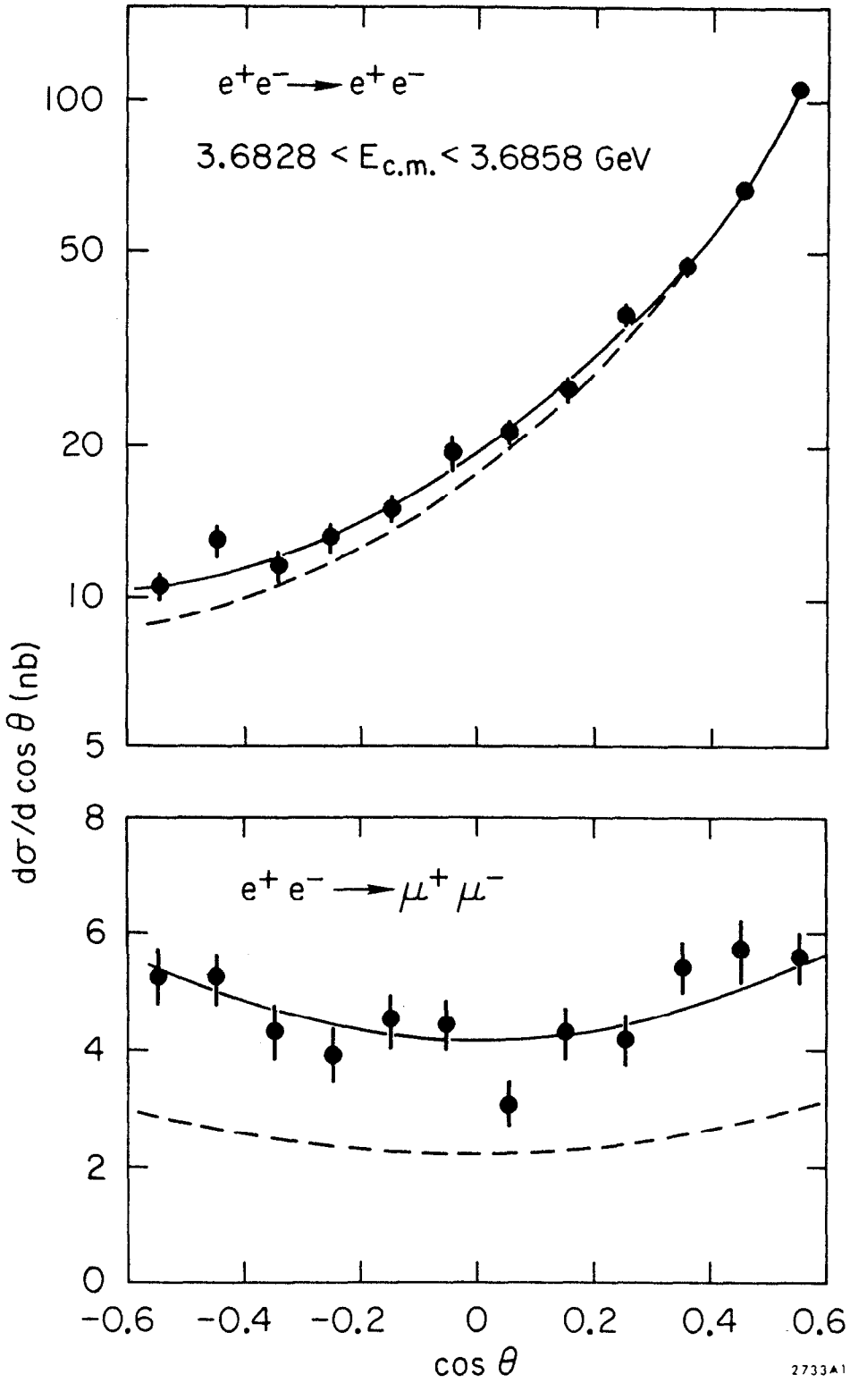
$e^+e^- \rightarrow e^+e^-$
$3.6828 < E_{c.m.} < 3.6858$ GeV
100
50
20
10
5
$d\sigma/d\cos\theta$ (nb)
$e^+e^- \rightarrow \mu^+\mu^-$
8
6
4
2
0
-0.6
-0.4
-0.2
0
0.2
0.4
0.6
$\cos\theta$
2733A1

Fig. 19

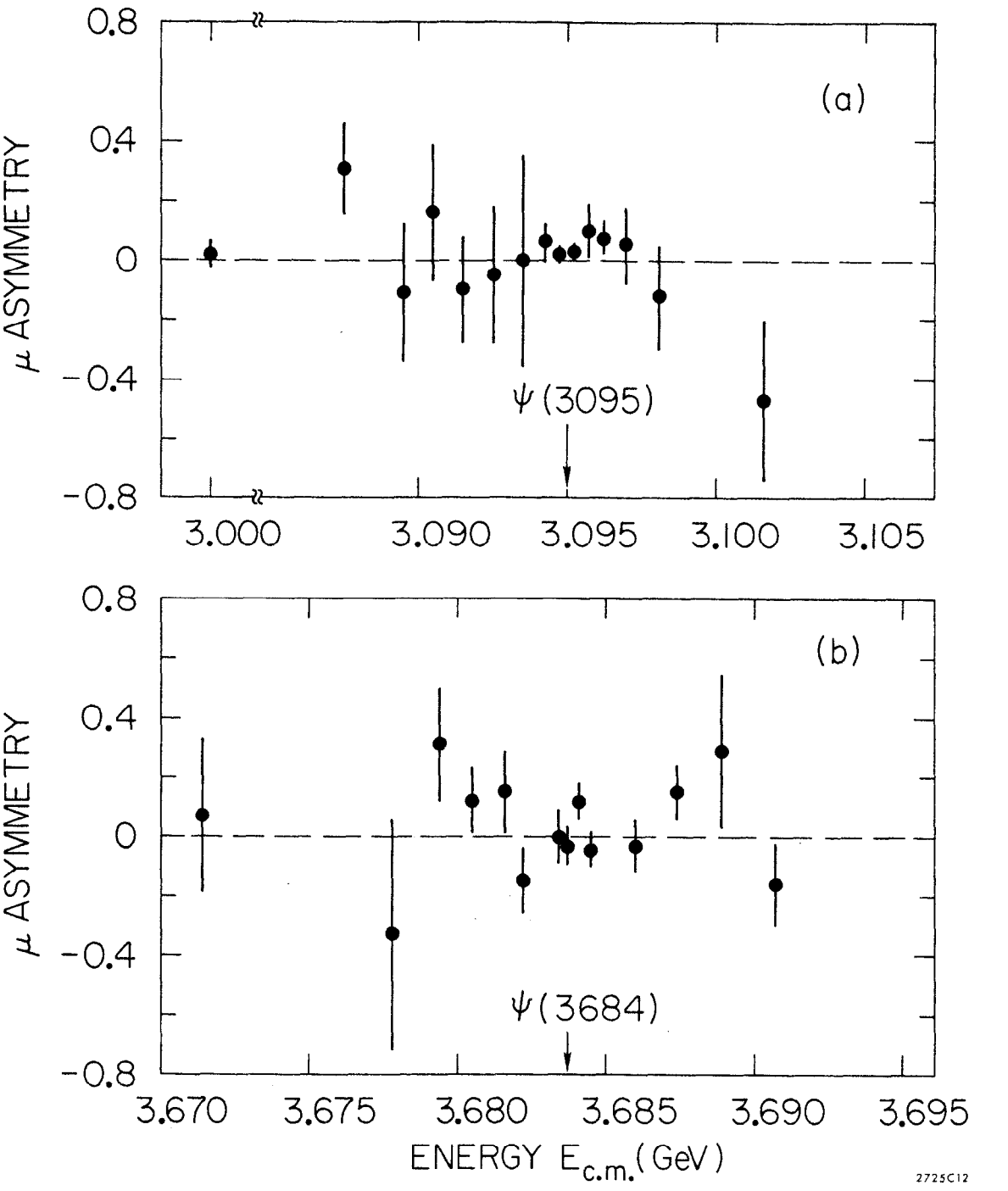
0.8
0.4
0
-0.4
-0.8
μ ASYMMETRY
(a)
ψ(3095)
3.000
3.090
3.095
3.100
3.105
0.8
0.4
0
-0.4
-0.8
μ ASYMMETRY
(b)
ψ(3684)
3.670
3.675
3.680
3.685
3.690
3.695
ENERGY E c.m. (GeV)
2725C12

Fig. 20

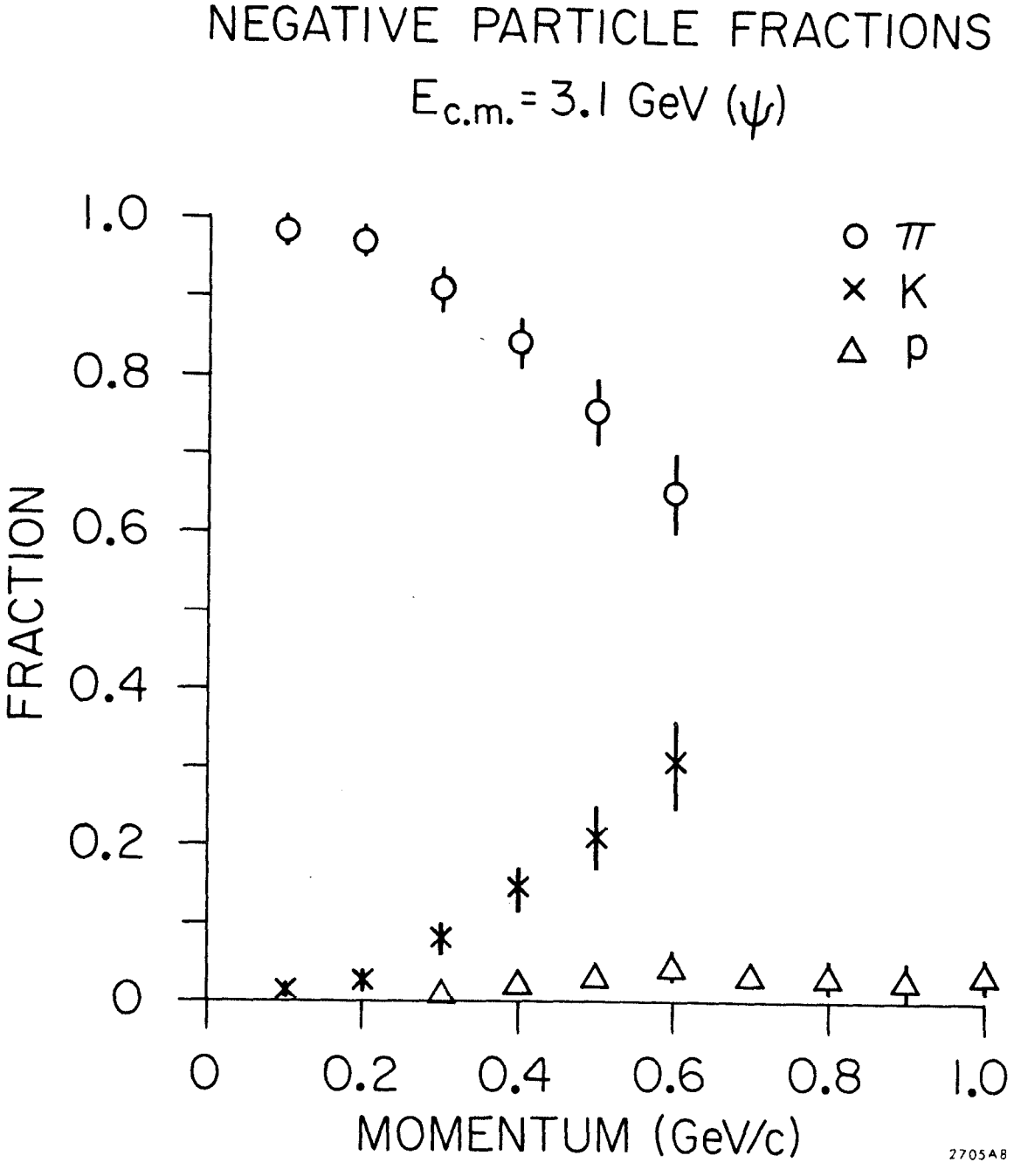
NEGATIVE PARTICLE FRACTIONS
$E_{c.m.} = 3.1$ GeV (ψ)
FRACTION
MOMENTUM (GeV/c)
π
K
p
1.0
0.8
0.6
0.4
0.2
0
0.2
0.4
0.6
0.8
1.0
2705A8

Fig. 21

MULTIPION FINAL STATE

$$\alpha = \frac{R_{ON}}{R_{OFF}} = \frac{\sigma^{H}_{ON}/\sigma^{\mu}_{ON}}{\sigma^{H}_{OFF}/\sigma^{\mu}_{OFF}}$$

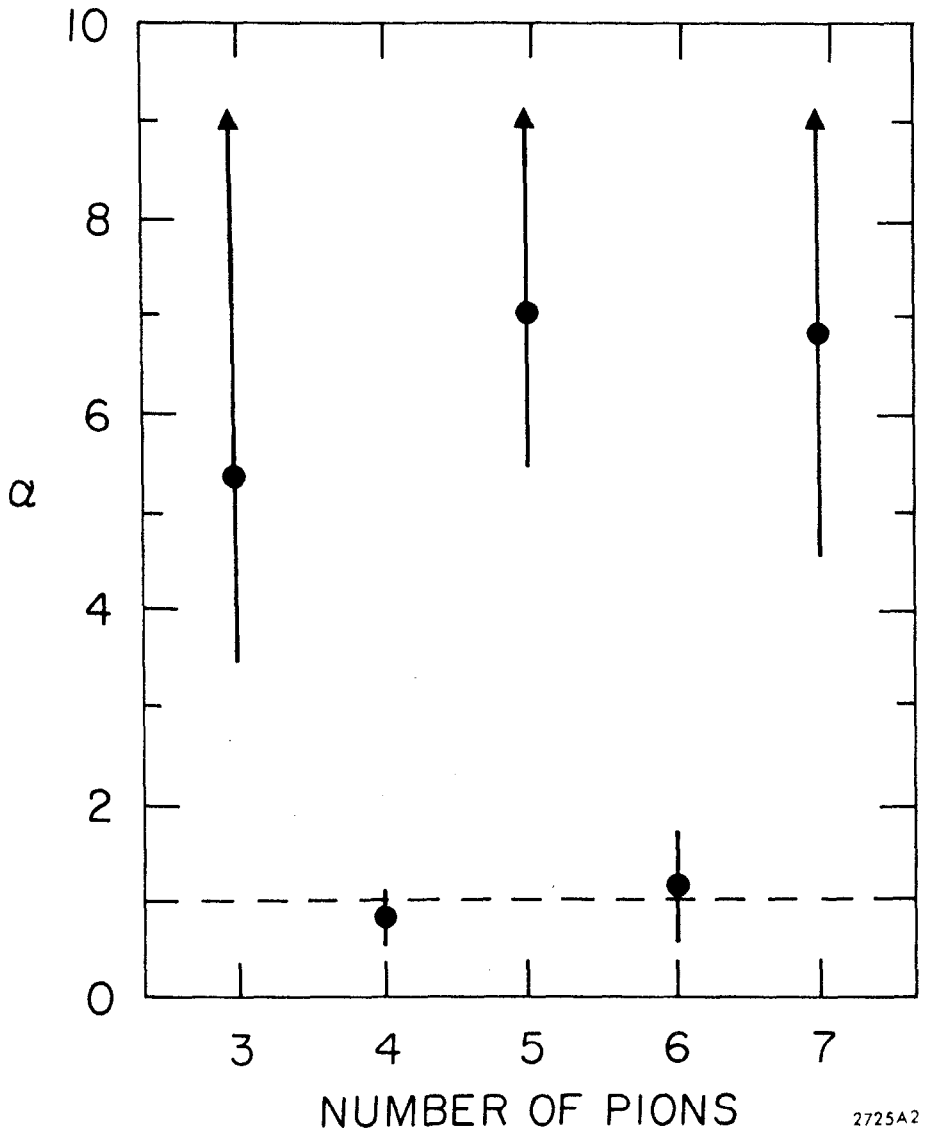

Fig. 22

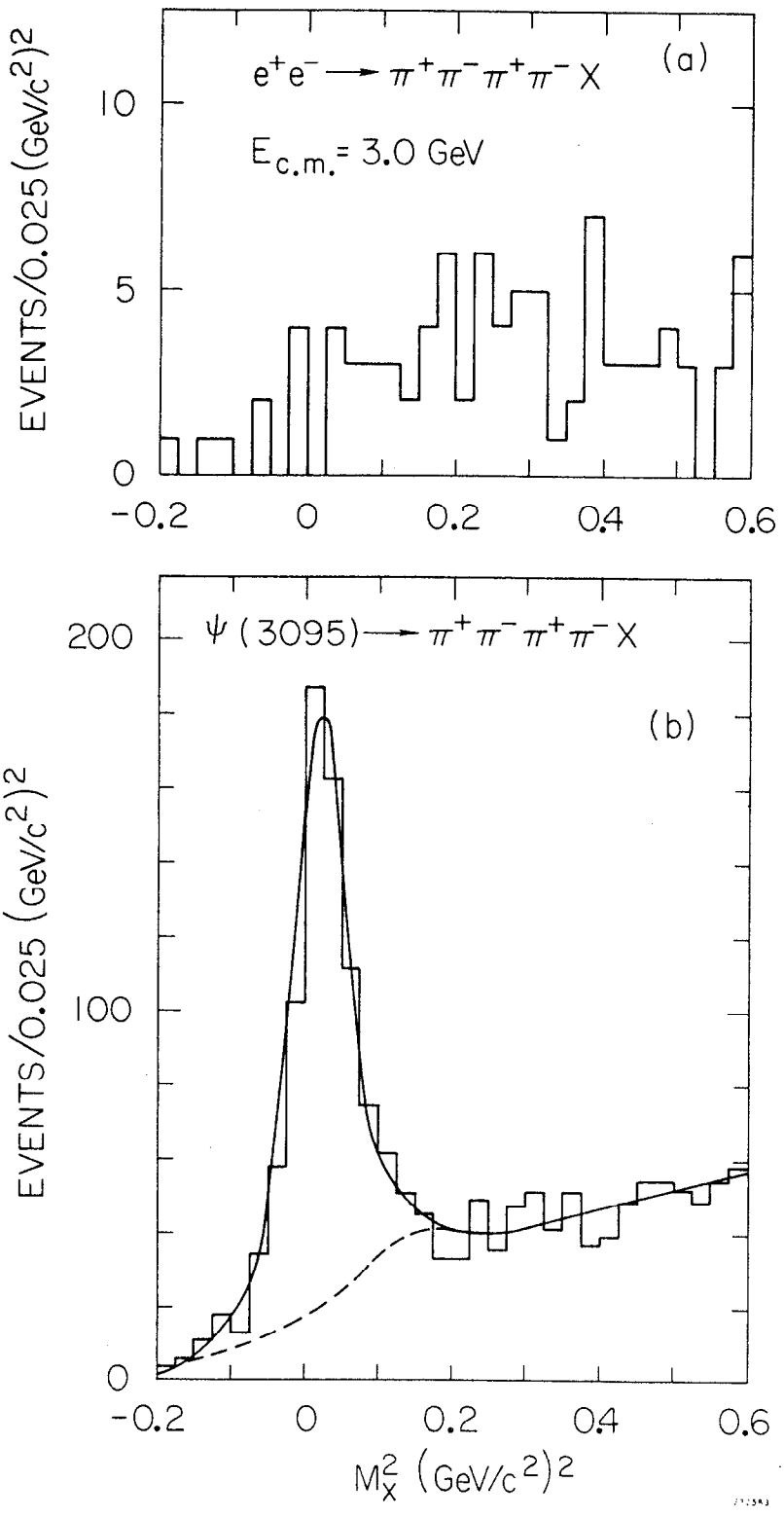
$e^+e^- \rightarrow \pi^+\pi^-\pi^+\pi^- X$
(a)
$E_{c.m.}$ = 3.0 GeV
EVENTS/0.025 (GeV/c²)²
10
5
0
-0.2
0
0.2
0.4
0.6
ψ (3095) $\rightarrow \pi^+\pi^-\pi^+\pi^- X$
(b)
200
100
0
M_X^2 (GeV/c²)²

Fig. 23

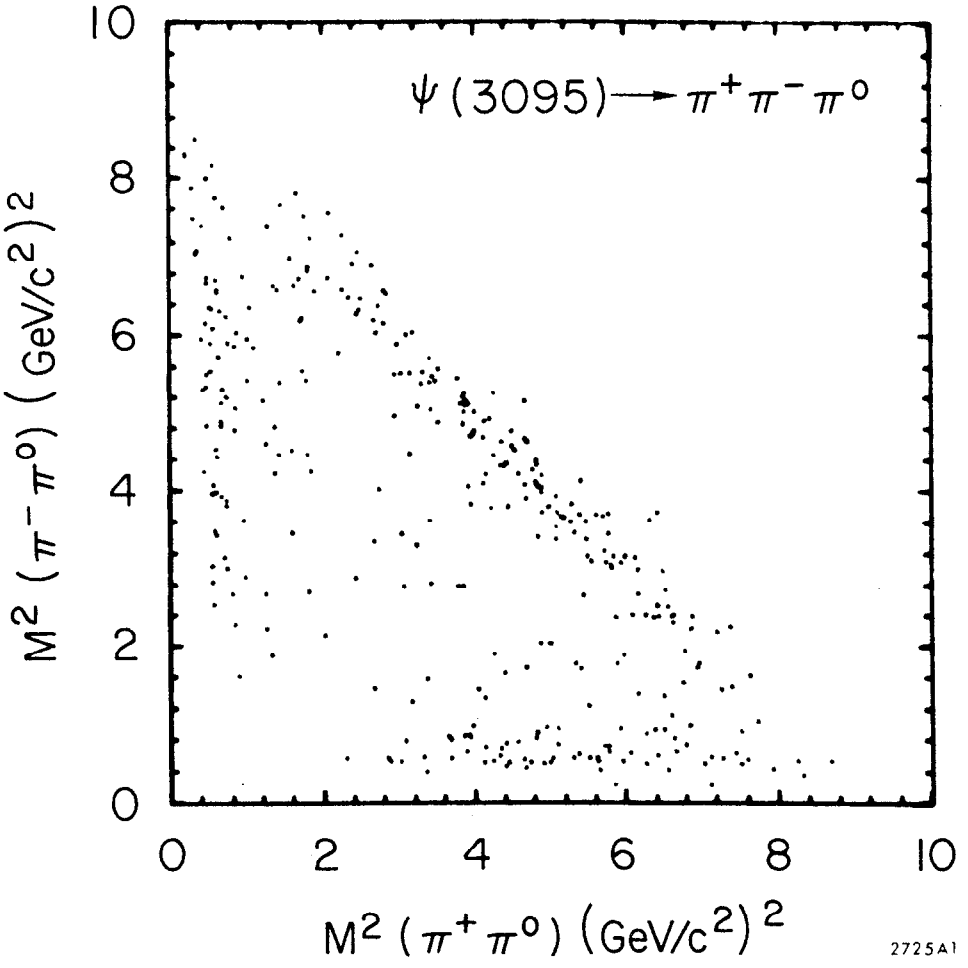

Fig. 24

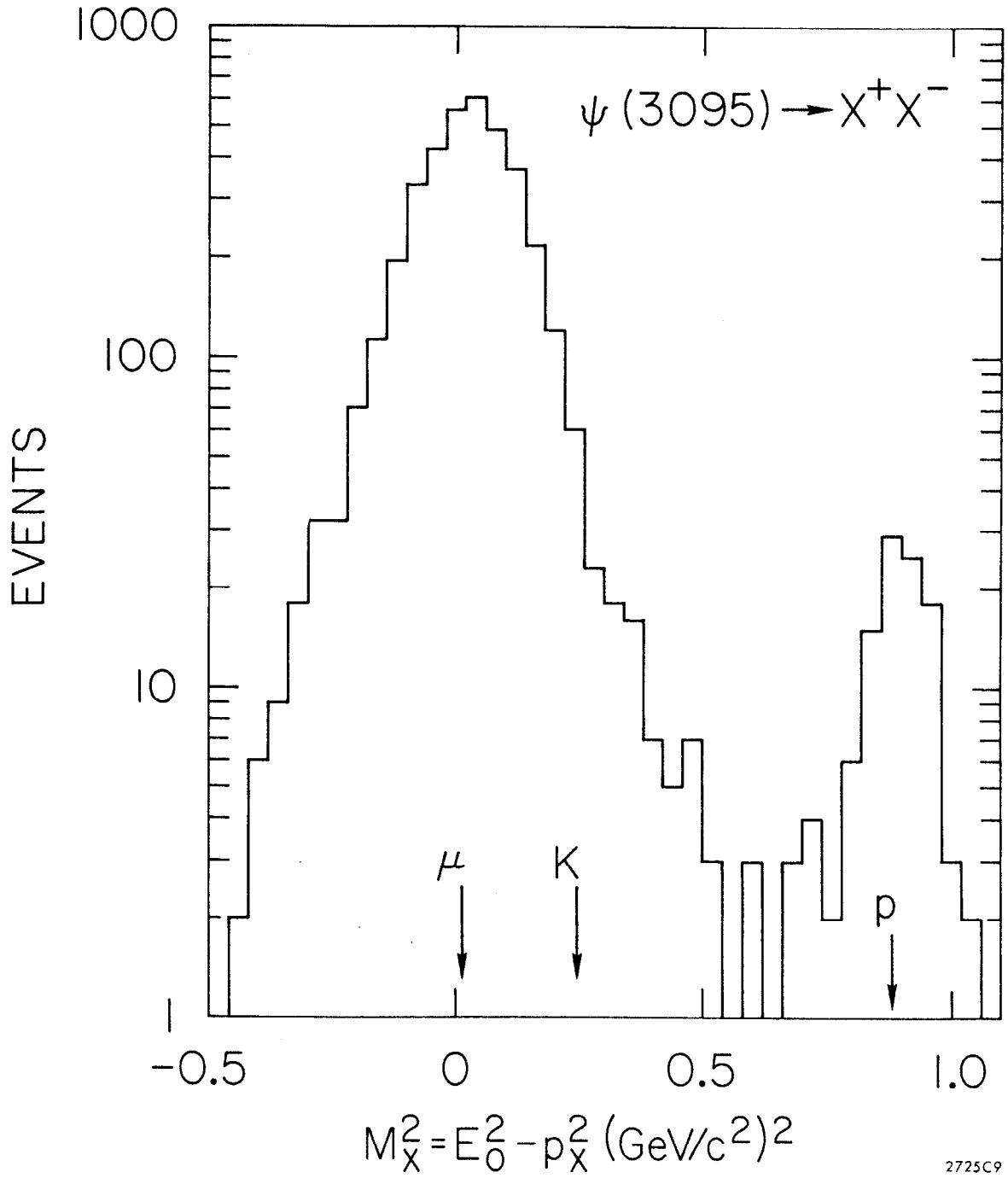
1000
100
10
1
EVENTS
ψ(3095) → X⁺X⁻
μ
K
p
-0.5
0
0.5
1.0
M²X = E²0 - p²X (GeV/c²)²
2725C9

Fig. 25

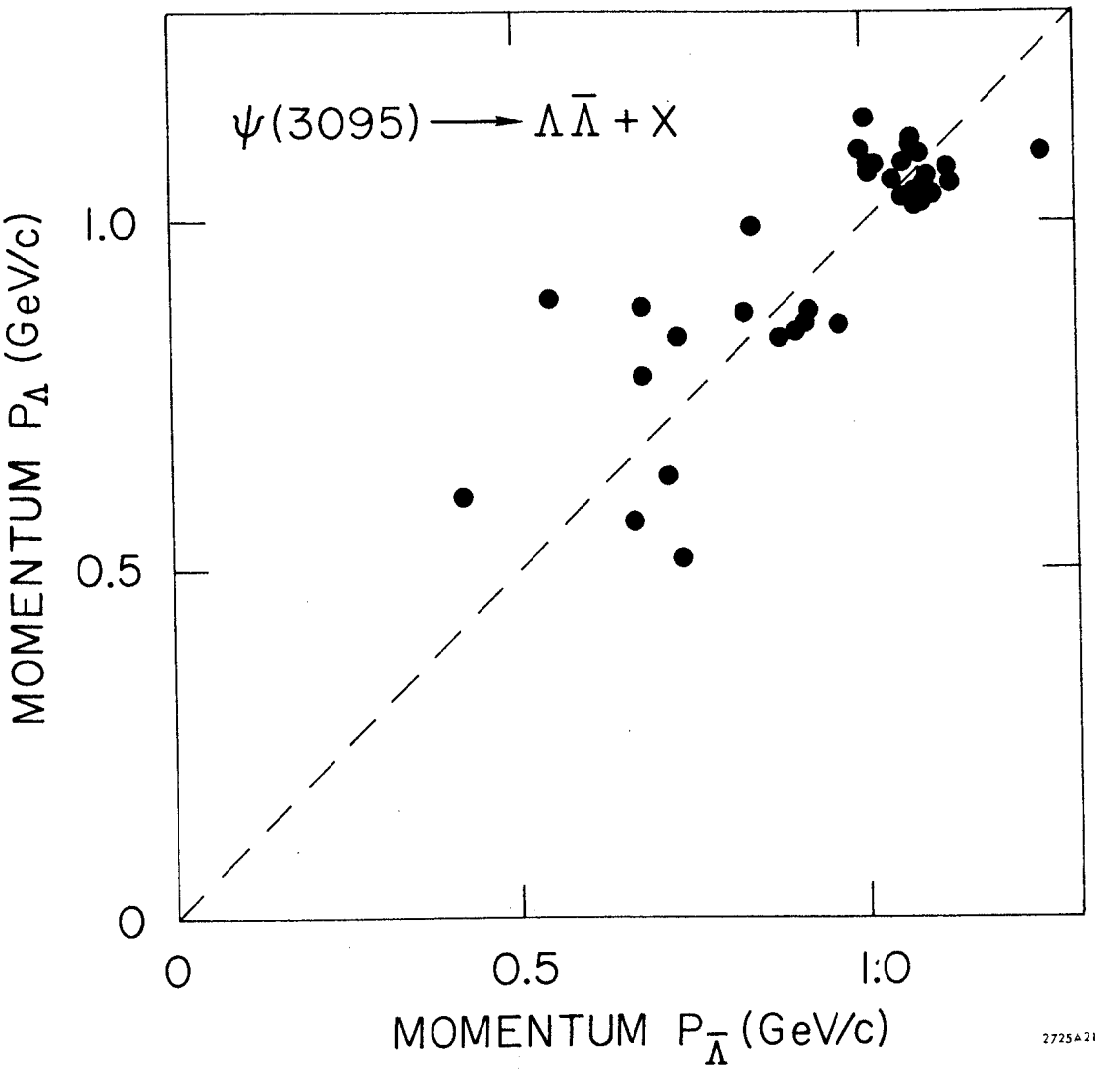
ψ(3095) ⟶ Λ Λ̄ + X
MOMENTUM P_Λ (GeV/c)
1.0
0.5
0
0
0.5
1.0
MOMENTUM P_Λ̄ (GeV/c)
2725A21

Fig. 26

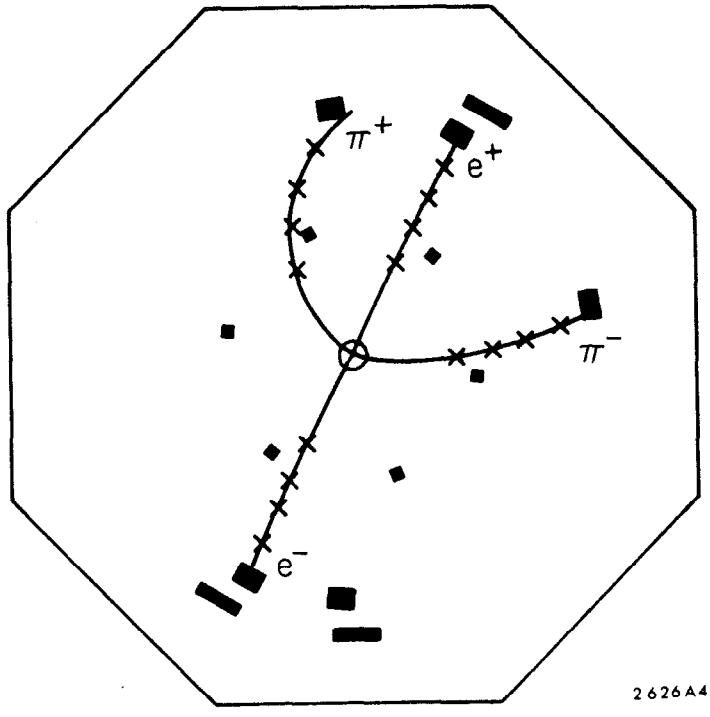
π^+
e^+
π^-
e^-
2626A4

Fig. 27

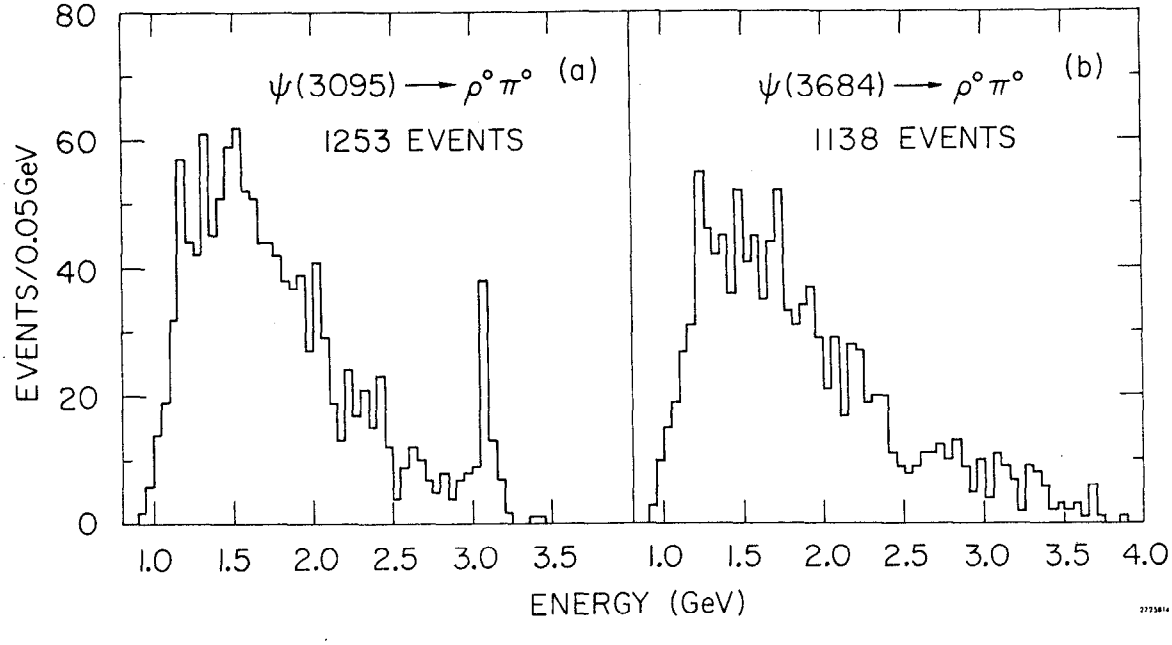
80
60
40
20
0
EVENTS/0.05GeV
$\psi(3095) \rightarrow \rho^\circ\pi^\circ$ (a)
1253 EVENTS
$\psi(3684) \rightarrow \rho^\circ\pi^\circ$ (b)
1138 EVENTS
1.0 1.5 2.0 2.5 3.0 3.5
1.0 1.5 2.0 2.5 3.0 3.5 4.0
ENERGY (GeV)

Fig. 28

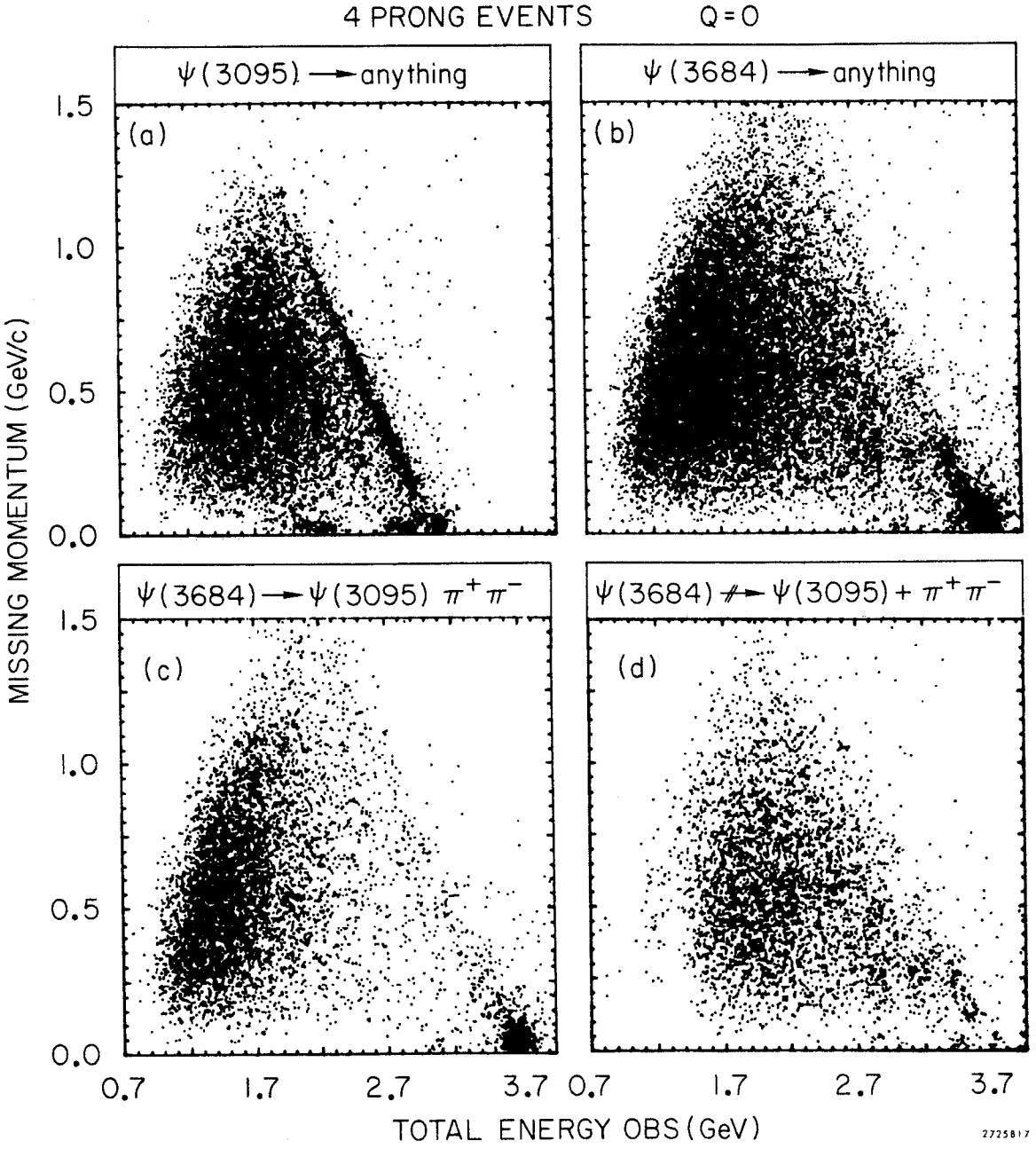
4 PRONG EVENTS
Q=0
ψ(3095) → anything
ψ(3684) → anything
(a)
(b)
ψ(3684) → ψ(3095) π⁺π⁻
ψ(3684) ↛ ψ(3095) + π⁺π⁻
(c)
(d)
MISSING MOMENTUM (GeV/c)
1.5
1.0
0.5
0.0
0.7
1.7
2.7
3.7
TOTAL ENERGY OBS (GeV)
2725B17

Fig. 29